

AN ABSTRACT OF THE THESIS OF

Joseph Paul Hennessey, Jr. for the degree Master of Science  
(Name)

in Atmospheric Sciences presented on July 24, 1974  
(Major Department) (Date)

Title: A STUDY OF THE VARIATION OF THE SURFACE  
ROUGHNESS LENGTHS AT RISØ, DENMARK

Abstract approved: **Redacted for privacy**  
Ernst W. Peterson

The Risø data were analyzed for variations in the surface roughness lengths. The method of analysis was tested on the Wangara data and proved satisfactory at this homogeneous site.

Annual mean surface roughness lengths were determined for three wind speed categories and three stability categories. The decrease in surface roughness length with increasing wind speed and decreasing stability was large but not generally statistically significant because of the large dispersion in the data. The annual mean roughness length varied over several orders of magnitude.

These results and also the ten year mean profiles were compared with those of previous investigators.

It was found that the standard deviation determined from mean annual profiles over a ten year period was greater than one order of magnitude.

A Study of the Variation of the Surface Roughness  
Lengths at Risø, Denmark

by

Joseph Paul Hennessey, Jr.

A THESIS

submitted to

Oregon State University

in partial fulfillment of  
the requirements for the  
degree of

Master of Science

Completed August 1974

Commencement June 1975

APPROVED:

Redacted for privacy

\_\_\_\_\_  
Professor of Atmospheric Sciences  
in charge of major

Redacted for privacy

\_\_\_\_\_  
Chairman of Department of Atmospheric Sciences

Redacted for privacy

\_\_\_\_\_  
Dean of Graduate School

Date thesis is presented July 24, 1974

Typed by Cheryl E. Curb for Joseph Paul Hennessey, Jr.

## ACKNOWLEDGEMENTS

I wish to thank Professor Fred W. Decker for his valuable assistance in editing the manuscript. Thanks are also due to Kenneth Key for his many constructive criticisms and to Leta Andrews for her timely review of the manuscript.

Special thanks are due to Dr. Ernest W. Peterson, without whose advice, assistance, and support this thesis would have been impossible.

This research was supported by the National Science Foundation under Grant GA-31269. The Oregon State University Computing Center provided part of the computing time.

## TABLE OF CONTENTS

<u>Chapter</u>		<u>Page</u>
I	INTRODUCTION	1
II	LITERATURE REVIEW	3
III	RICHARDSON NUMBERS	17
IV	TEST OF THE METHOD OF SELECTING NEUTRAL PROFILES AT A HOMOGENEOUS SITE	23
V	DATA AND SITE DESCRIPTION	28
VI	REDUCTION OF THE OBSERVATIONS	31
VII	TEN YEAR MEAN PROFILES	36
VIII	ANNUAL AND SEASONAL VARIATION OF THE SURFACE ROUGHNESS LENGTHS	48
IX	CONCLUSIONS	63
	BIBLIOGRAPHY	65
	APPENDIX A: DERIVATION OF THE LOGARITHMIC WIND PROFILE	70
	APPENDIX B: ANALYSIS OF METEOROLOGICAL DATA	80
	APPENDIX C: TYPICAL SURFACE ROUGHNESS LENGTHS	85

## LIST OF TABLES

<u>Table</u>		<u>Page</u>
1	Values of fetch and height for 90 percent adjustment of profiles.	6
2	Comparison of the Wangara neutral profiles selected by various methods.	26
3	Comparison of the values of $z_0$ found by previous investigators at Risø.	32
4	Comparison of the values of $z_0$ (from ten year mean profiles) found by previous investigators with those found by this study.	34
5	Comparison of roughness lengths computed from the ten year mean profiles by (1) extrapolating from the 7 and 23 m heights, (2) extrapolating from the 23 and 39 m heights, and (3) fitting a least squares fit to these three heights.	44
6	Statistics for annual mean value of $\ln(z_0)$ computed from neutral profiles for each wind speed category.	58
7	Statistics for annual mean values of $\ln(z_0)$ computed from wind speed category 1 profiles for each Richardson number category.	59
8	Statistics for annual mean values of $\ln(z_0)$ computed from wind speed category 2 profiles for each Richardson number category.	60
9	Statistics for the ten year variation of seasonal mean values of $\ln(z_0)$ computed from neutral, mean seasonal profiles and then averaged over all speed categories.	62

## LIST OF FIGURES

<u>Figure</u>		<u>Page</u>
1	Roughness length non-dimensionalized by the roughness length for neutral conditions versus the stability parameter.	4
2	The effect of the roughness elements on the structure of the flow near the ground for (a) stable, and (b) unstable conditions.	4
3	Dependence of $\ln(z_0)$ on surface friction velocity for (1) an aerodynamically smooth wall, and (2) sea surface.	8
4	Roughness length versus stability ratio.	15
5	Map of eastern Denmark.	29
6	Map of Risø and vicinity.	30
7	Map of Risø area showing Panofsky and Petersen's Classes A, B, and C and the direction groups 1-8 of this study.	35
8	Ten year mean profiles averaged over all wind speeds.	38
9	Form of the wind profile over a surface of roughness $z_0$ , in lapse, neutral, and stable conditions, plotted against a logarithmic height scale.	39
10	Ten year mean profiles selected by Petersen's method, Panofsky and Petersen's method, and the method of this study. Wind directions $85^\circ$ - $225^\circ$ , $225^\circ$ - $005^\circ$ .	40
11	Comparison by superposition of the curvature of the ten year mean profiles selected by the Peterson method and by the Panofsky and Petersen method.	41

LIST OF FIGURES (Cont.)

<u>Figure</u>		<u>Page</u>
12	Schematic of the simplest inhomogeneity problem - a singular, one dimensional change in surface roughness.	41
13	Ten year mean profiles selected by Peterson's method, Panofsky and Petersen's method, and by the method of this study. Wind direction 225°-245°.	46
14	Map of Risø showing azimuthal distribution of surface roughness lengths.	47
15-22	Annual variation of roughness lengths computed from the mean, annual neutral profiles for Groups 1-8, respectively.	49- 56

## LIST OF SYMBOLS

A	total horizontal area of the upstream fetch
$c_p$	specific heat of dry air at constant pressure
$\delta_e$	height of equilibrium layer
$\delta_i$	height of internal boundary layer
$\epsilon$	stability parameter
$\Gamma$	$g/c_p$ , adiabatic lapse rate
g	acceleration due to gravity
h	mean height of the roughness elements
H	$c_p \rho \overline{W'T'}$ , turbulent heat flux
L	$-u_*^3 c_p \rho \theta / \kappa gH$ , Monin-Obukhov length scale
l	eddy length scale
$\kappa$	von Karman's constant
n	total number of roughness elements in upstream fetch
q	specific humidity
$\rho$	surface air density
Ri(z)	gradient Richardson number evaluated at height z
R	stability ratio
s	silhouette area of average obstacle
S	A/n, specific area
T	ambient air temperature
$\Theta$	mean potential temperature of an adiabatic atmosphere
$\theta$	$T + \Gamma z$ , potential temperature

LIST OF SYMBOLS (Cont.)

$\tau_0$	surface stress
$u$	mean horizontal wind speed
$u_z$	mean horizontal wind speed at height $z$ meters
$u_*$	$(\tau_0/\rho)^{1/2}$ , surface friction velocity
$W'$	vertical velocity fluctuations
$x, z$	horizontal and vertical space coordinates
$z_0$	surface roughness length
$z_{i,j}$	geometric mean height between tower levels $i$ and $j$
$z_i, \theta_i,$	$z, \theta, u$ at the $i^{\text{th}}$ tower level
$u_i$	

# A STUDY OF THE VARIATION OF THE SURFACE ROUGHNESS LENGTHS AT RISØ, DENMARK

## I. INTRODUCTION

The laws for the velocity distribution within the lower part of the planetary boundary layer (PBL) have been verified experimentally. In the case of neutrally stratified (adiabatic) flow over homogeneous terrain, the wind profile is logarithmic (Appendix A):

$$u_z = (u_*/\kappa)\ln(z/z_0) \quad (1-1)$$

where  $u_*$  is the surface friction velocity,  $\kappa$  is von Karman's constant, and  $z_0$  is the surface roughness length.

The surface roughness length is not only a boundary condition for Equation 1-1 but also the length scale for the surface layer. Unfortunately, there is as yet no a priori way to precisely determine it without recourse to experiment.

Numerous careful boundary layer studies such as the Wangara expedition (Clarke et al., 1971) have shown that it is possible to accurately compute  $z_0$  from Equation 1-1 at a homogeneous site.

By averaging many observations over broad direction sectors, Slade (1969) was able to compute  $z_0$  at a very inhomogeneous site. This success was encouraging since no well instrumented operational tower is located at a completely homogeneous site.

In the last two years considerable work has been done on the ten year record from the micrometeorological tower of the Danish Atomic Energy Commission (AEK) at Risø, Denmark (Panofsky and Petersen, 1972; Petersen and Taylor, 1973; Carl et al., 1973; Peterson, 1974a). This site with its complex terrain seems especially interesting for studying profiles over inhomogeneous terrain; however, the results have been contradictory. Peterson computed  $z_0$ 's significantly lower than either Panofsky and Petersen or what would have been expected from the physical description of the site (Appendix C). Petersen and Taylor, using the method of Panofsky and Petersen, reported unexpectedly low values of  $z_0$  for the sea surface in one sector.

The objectives of this study are threefold:

1. To determine whether or not Slade's hypothesis can be applied to the operational data from the Risø tower.
2. To investigate further the apparently conflicting results of Peterson with those of Panofsky and Petersen.
3. To determine the precision to which the surface roughness lengths can be estimated at Risø.

## II. LITERATURE REVIEW

The bulk of the literature on surface roughness lengths has been published since 1960. Laikhtman (1961) attempted to synthesize what was then known about the physics of the planetary boundary layer. He concluded from the results of many studies that  $z_0$  is proportional to the average dimensions of the individual roughness elements with a constant of proportionality varying from 1/5 to 1/100. A small constant of proportionality is usually associated with small, well-streamlined roughness elements and a large constant with large, angular ones.

Laikhtman also summarized the little known results of T. A. Ogneva (1955) who studied the explicit dependence of the surface roughness length on stratification. Ogneva used a dimensionless stability parameter,  $\epsilon$ , where  $\epsilon = \epsilon(z_0/L)$ .  $\epsilon$  is a function of  $z_0/L$  because this is the only possible non-dimensional combination of the surface layer parameters  $L$ ,  $u_*$ , and  $z_0$ . Neutral stratification occurs when  $\epsilon = 0$ , stable stratification at  $\epsilon > 0$ , and unstable stratification at  $\epsilon < 0$ . Figure 1 shows Ogneva's unexpected result -- surface roughness decreasing with increasing stability. This could be explained away as the result of an inadmissible extrapolation from the velocity profiles but Laikhtman had a physical interpretation of this effect which is illustrated by Figure 2. This figure shows how

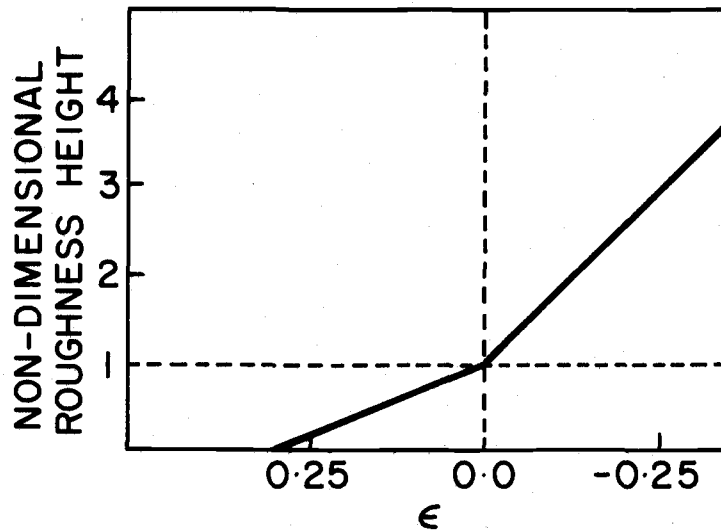


Figure 1. Roughness length non-dimensionalized by the roughness length for neutral conditions versus the stability parameter,  $\epsilon$ . After Laikhtman (1961).

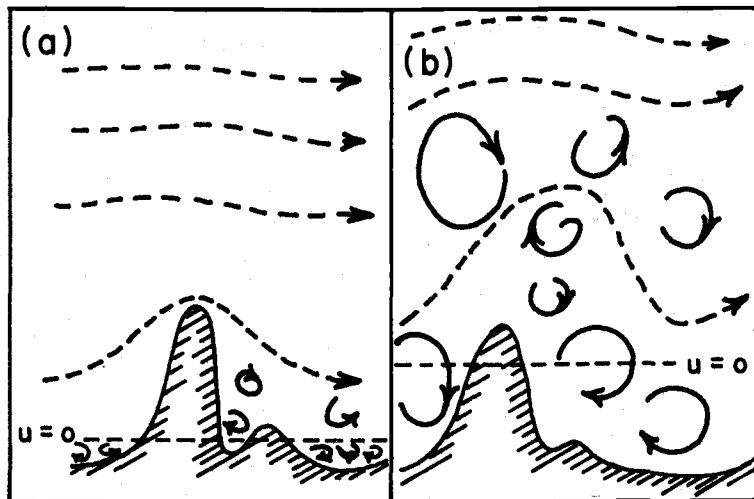


Figure 2. The effect of the roughness elements on the structure of the flow near the ground for (a) stable, and (b) unstable conditions ( $u = 0$  at  $z = z_0$ ). After Laikhtman (1961).

the breakup of the flow in the vortices near the height  $z=z_0$  is connected with the flow over individual roughness elements resulting in  $u=0$  at  $z=z_0$ . This breakup is hampered by stable conditions and therefore takes place in a relatively thin layer (Figure 2a); on the other hand, non-stable conditions contribute to a much larger layer (Figure 2b).

Tanner (1963) summarized the existing rules of thumb that could then be used to determine the fetch and sampling height requirements from wind profiles over effectively homogeneous terrain:

1. The highest instrument level should not exceed approximately 1/50 of the upwind distance from significant discontinuities in surface structure. (A fetch of at least 2,000 m would be required to meet this requirement at Risø.)
2. The downwind distance that the influence of obstacles such as rows of trees, buildings, etc., is felt is at least eight times the height of the obstacle and this distance should be added to the fetch requirements.
3. After a minimum fetch of 10 m, Elliott's (1958) equation can be used:

$$\delta_i = 0.75 x^{0.8} \quad (h \text{ and } x \text{ in cm}) \quad (2-1)$$

For a height,  $\delta_i$ , of 2 m, the required fetch would be 1080 m.

Dyer (1963) calculated the fetch requirements for 90% adjustment of the temperature and humidity profiles over a discontinuity in surface temperature and humidity (e. g., a coastline) without considering the further complication of a roughness discontinuity. His results are summarized by the following table.

Table 1. Values of fetch and height for 90% adjustment of profiles. After Dyer (1963).

Height (m)	Fetch (m)	Fetch-height ratio
0,5	70	140
1	170	170
2	420	210
5	1350	270
10	3300	330
20	8100	405
50	26500	530

Monteith (1963) has summarized the changes in  $z_0$  with wind speed for surfaces covered with vegetation as follows:

1. For vegetation with small leaves, leaf drag coefficients decrease with wind speed fast enough to offset the effect of leaf flutter;  $z_0$  decreases with wind as observed in grass, lucerne, and beans.
2. Drag on larger leaves is dominated by the effects of flutter, and streamlining is unimportant at normal wind speeds;  $z_0$  increases with increasing fluttering and hence with wind speed as observed for maize.
3. For leaves of intermediate size,  $z_0$  increases with wind speed in the region of leaf flutter, but decreases at higher wind speeds in the region of streamlining as observed for wheat and rice.

O'Brien (1964) studied 337 neutral profiles using data from two mobile micrometeorological stations near Dallas, Texas. The neutral profiles were selected by the temperature lapse rate below 5 m, and the surface roughness lengths were determined from the least squares fit to the four data points below 5 m. The use of these four points from the layer closest to the surface instead of all eight available points resulted in less dispersion in the estimates of  $z_0$ . After eliminating special cases of low wind speed and extremes of stability, O'Brien found that the variations of  $z_0$  could be explained as a function of the seasonal variation in the size of the surface roughness elements and were not a function of wind direction or speed except in one sector which felt the effects of an obstacle 100 yards upstream. The magnitudes of the surface roughness for this site agreed with the results of previous investigators for grass covered sites (Appendix C).

Kitaygorodskiy and Volkov (1965) reanalyzed all available data on the surface roughness height over a sea surface and were able to account for the large variation in the observed roughness lengths. Their results are summarized by Figure 3.

Plate and Lin (1966) simulated neutral profiles in a wind tunnel. Their data showed rather large changes of  $z_0$  with stratification; however, since they did not need to specify  $z_0$  explicitly, this variation was not investigated. They argued that there was no reason to assume that  $z_0$  is affected by thermal stratification since it is

determined by the flow closest to the ground where stratification has essentially no effect on the flow field. This argument is no longer reasonable in view of the theoretical advance by Tennekes (Appendix A).

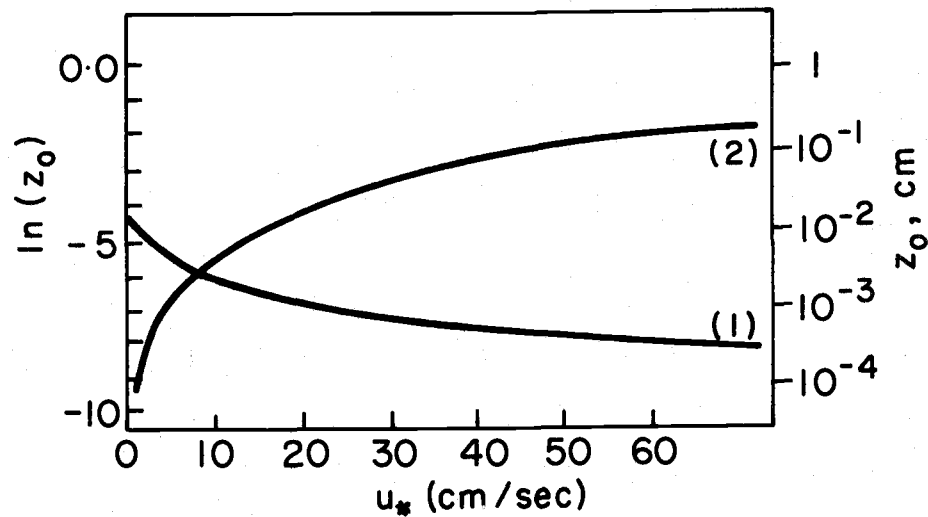


Figure 3. Dependence of  $\ln(z_0)$  on surface friction velocity for (1) an aerodynamically smooth wall, and (2) sea surface. After Kitaygorodskiy and Volkov (1965).

Lettau (1969) has approached the problem of estimating  $z_0$  based on a visual inspection of the site and measurement of characteristic roughness elements. He proposed the following equation:

$$z_0 = 0.5 hs/S \quad (2-2)$$

where  $h$  is the effective obstacle height,  $s$  is the silhouette area of the average obstacle, and  $S$  is the specific area ( $\text{cm}^2/\text{roughness}$ )

element). Lettau used this equation a priori to estimate the roughness length for the field study at Davis, California, in 1967. His value agreed with the a posteriori calculation from the profile data to within an order of magnitude.

Slade (1969) analyzed 1965 and 1967 data from a TV tower which was situated in rough, irregular terrain near Philadelphia. The area surrounding the tower was covered with trees, fields, and a variety of residential structures. All instruments were above 12.2 m and the data was automatically averaged over ten minute periods. Neither the number of neutral profiles nor the method of selecting individual neutral profiles was published; however, it can be inferred that these were selected on the basis of the temperature lapse rate alone. The surface roughness length ranged from 22 cm for the southerly sector to 3.1 m for the northerly sector and were what could have been predicted from a visual inspection of the site (Appendix C). His results are as follows:

1. Extrapolating from the 12.2-30.5 m segment of the profile resulted in a  $z_0$  twice as large as that computed from the profile segment 30.5-61.0 m in the southerly sector, but there is no significant difference in the northerly sector.
2. Averaging over a broad direction sector made it likely that the flow in the lee of any one obstacle would not unduly affect the average profile.

3. The concave down curvature in the southerly neutral profiles may be evidence of a complex internal boundary layer structure.
4. The wind speed profiles at an irregular site differ quite radically depending on the local upstream terrain.
5. Technique and concepts developed for the PBL over regular terrain seem to be applicable in a deep layer over quite rough and irregular terrain.
6. It may be possible to obtain representative wind profiles in highly irregular terrain by averaging many observations over a broad direction sector.

Blackadar et al. (1969) analyzed data from a 150 m meteorological tower on Merritt Island at the Kennedy Space Center which was situated three miles from the Atlantic Ocean in a well-exposed area free from the interfering effects of nearby structures. There was considerable azimuthal variation in the roughness elements, which included homogeneous sectors with low vegetation, sectors with 200 or 450 m fetches of low vegetation running into forests, and one sector with a body of water after a 225 m fetch of low vegetation. The low vegetation was  $1-1\frac{1}{2}$  m tall and the trees were 10-15 m tall. The stability was determined from a gradient Richardson number computed from a form of Equation 3-9. The surface roughness was computed for 176 cases from the equation for the nonstable wind profile and then categorized as near-neutral or unstable. Their results are as

follows:

1. The roughness determined from a near-neutral wind profile is more reliable than the one obtained from an unstable profile. This is due to the uncertainty in the gradient Richardson number.
2. There is some scatter of  $z_0$  in every sector, but the roughness length is independent of stability and wind speed.
3. The  $z_0$ 's in this study were compatible with those previously computed by Fichtl (1968) for the same site.
4. Large variation in the gradient Richardson number yield similar values of roughness length.
5. Computing  $z_0$  from an averaged wind profile minimizes the effects of errors attributable to sensors and calculation techniques.
6. The determination of  $z_0$  is generally most accurately done from the two or three lowest levels of observation.

Echols (1970) studied the effects of a coastline on the boundary layer wind structure with a 32 m tower 90 m inland from the upper Texas coast. The terrain was a flat and very homogeneous coastal marsh overgrown with marsh and salt grasses varying in height from 10 to 45 cm. Two days' data from June 1968 were analyzed. On these days there were long periods of steady onshore flow nearly perpendicular to the shoreline. Measurements were made at five heights between 1 m and 27 m. Neutral profiles were selected primarily on the basis of Deacon number. The results are as follows:

1. The mean profiles were bent concave up with a kink at about 6.7 m which was interpreted as the top of the internal boundary layer formed by the onshore flow.
2. Nighttime roughness values were somewhat higher than the daytime values.
3. The roughness of the water surface as computed from the tower data above the kink was very small (0.0001 to 0.0003 cm).
4. The roughness of the beach was computed from the tower data below the kink and was in agreement with what could have been expected from the physical description of the site.

Sanders and Weber (1970) analyzed April through July data from a TV tower in a relatively undeveloped area near Oklahoma City. The terrain was gently undulating open fields and pastures. Wooded areas with trees 15-25 ft tall were confined to shallow gullies, drainage areas and ponds. The nearest trees were 100-500 ft SSE of the tower. The three lowest sensors were mounted at 7.0, 44.5 and 90.2 m. The authors selected 128 neutral cases by Richardson number. No details of the selection process are given, but it can be inferred that some form of Equation 3-9 was used. Their results are as follows:

1. Since the lowest anemometer height was 7 m, the inclusion of a zero plane displacement would needlessly complicate calculations without improving the estimate of  $z_0$ .

2. The 7 m wind speed was the most difficult to fit to a logarithmic profile; in any case, the evaluation of the roughness length is uncertain because averaged profiles are seldom perfectly straight lines. Extrapolation from the lowest two levels resulted in unrealistically large roughness lengths, so it was necessary to use a least squares fit to the lowest three data points.
3. The mean values of  $z_0$  were similar to the typical values for similar surface conditions.
4. The sample sizes were too small to give a high degree of confidence in the mean value. The range was about one order of magnitude.

Sadeh et al. (1970) simulated neutrally stratified flow in a wind tunnel in order to study the effects of high roughness elements in the form of a model forest canopy with constant aerial density and little variation in the height of the individual roughness elements.

After the flow encountered the increased roughness at the leading edge of the canopy, three distinct regions developed. First appeared transition region 15 to 20 roughness heights wide, then a region of fully developed flow wherein both the mean velocity and the longitudinal turbulence intensity exhibited a state of relative equilibrium, and lastly a region of relatively small velocity increase caused by the change from rough to smooth which extended about five roughness heights downstream from the trailing edge of the canopy.

The velocity decrease characteristic of the flow field entering the region with high roughness elements extended to more than two roughness heights above the canopy, but its horizontal extent was only ten roughness heights downstream. This rate of decrease diminished with height above the canopy.

In the region of fully developed flow above the canopy where the wind profile was reasonably logarithmic, Sadeh found variation of  $z_0$  and  $u_*$  with height contradicting the assumption of constant shear stress.

Laboratory pipe flow studies have shown that, when the roughness elements are 0.8-6.7% of the boundary layer thickness,  $z_0$  and  $u_*$  are invariant with height. Sadeh showed that for roughness heights of 15% of the boundary layer thickness,  $z_0$  and  $u_*$  are variables. This is reasonable in view of the derivation in Appendix A.

Although the logarithmic wind profile is only strictly applicable to the region where  $z/z_0 \rightarrow \infty$ , it is often applied to regions closer to the ground. Van Hylckama (1970) studied the region above a homogeneous fetch of saltcedar ( $z/z_0 \approx 7$ ) with interesting results. A dense thicket of saltcedar exists in the flood plane of the Gila River near Buckeye, Arizona. The saltcedar was about 3 m tall, the fetch was 200 m in the prevailing wind direction and 100 m in the other directions. Instead of determining stability by the Richardson number, he used the stability ratio:

$$R = (T_{11} - T_5)/u_7^2 \quad (2-3)$$

where the subscripts refer to the height of the observation in meters.

He found:

1. The roughness lengths increased with increasing stability as shown in Figure 4.
2. Roughness lengths increased with increasing wind shear in the 4-7 m layer.
3. In 90% of all observed cases, the wind profiles in the first eight meters above the top of the saltcedar can be represented by the simple logarithmic Equation 1-1.

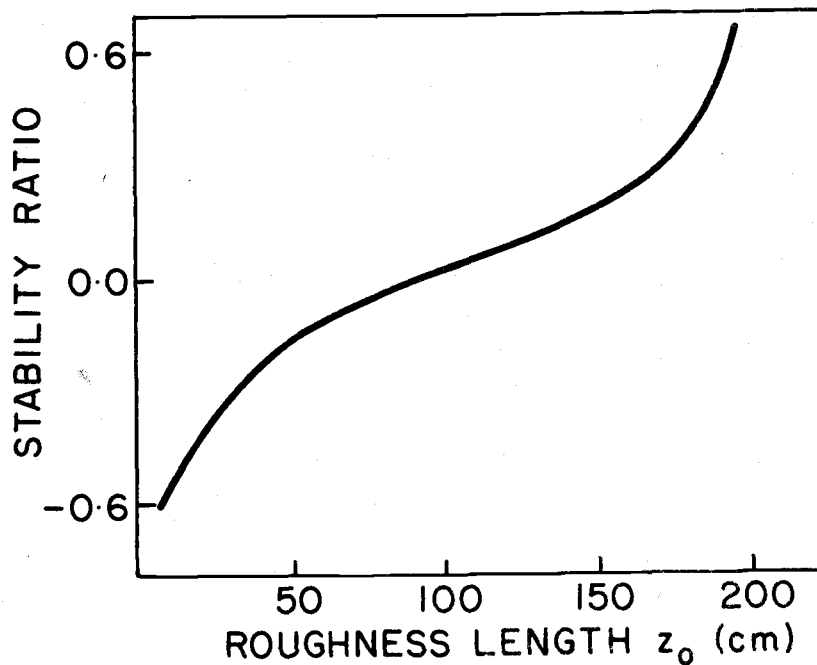


Figure 4. Roughness length versus stability ratio. After van Hylckama (1970).

Seginer et al. (1973) studied the interaction between atmospheric flow and windbreaks, two-dimensional porous roughness elements, in a field study in Israel. Gradient Richardson numbers were computed at the height of the windbreak (2.0 m) from the derivatives of the wind and temperature profiles at that level. Values of  $z_0$  were then computed from the logarithmic wind profile as well as for several diabatic models, and  $z_0$  was found to depend on stability, irrespective of how it was computed. The scatter of  $z_0$  near neutrality was relatively small, and the  $z_0$  computed from the logarithmic relationship showed the largest scatter, but this data was easiest to extrapolate to neutral conditions. The  $z_0$  determined in this manner was estimated to be within 50% of the true value.

## III. RICHARDSON NUMBERS

In order to compute the surface roughness lengths from Equation 1-1 it is essential to be able to select neutral profiles. Batchelor (1953) has shown that the Richardson number is the sole governing parameter for the class of flow systems consisting of low Mach number motion in a frictionless atmosphere in which the pressure and density everywhere depart by only a small fraction from the values for an equivalent atmosphere in adiabatic equilibrium and in which the vertical length scale of the velocity distribution is small compared to the scale height of the atmosphere. In doing so, he established that equality of Richardson numbers is the sufficient condition for dynamic similitude, verifying the empirical conclusions of Deacon (1949) and Pasquill (1949).

The gradient Richardson number is defined as:

$$Ri = (g/\Theta) [ (\partial\theta/\partial z)/(\partial u/\partial z)^2 ] \quad (3-1)$$

where  $g$  is the acceleration due to gravity,  $\theta$  is the potential temperature,  $\Theta$  is the mean potential temperature of an adiabatic atmosphere, and  $u$  is the horizontal wind velocity. This form of the Richardson number is used in applied meteorology because it can be readily estimated from profile variables.

Swinbank and Dyer (1968) used the simplest method of computing this parameter in their analysis of the Kerang data from the 1962-1964 CSIRO expeditions:

$$Ri = (g/\theta_1) [ (z_2 - z_1)(\theta_2 - \theta_1)/u_2 - u_1 ]^2 \quad (3-2)$$

where the layer  $(z_1, z_2)$  is the lowest layer with both temperature and wind speed measurements. This method was also used by Browne et al. (1970) in a study of the effects of terrain irregularities at a site in north central Arkansas.

Lettau (1957) has developed what seems to be the most frequently used method for making these computations. Using the transformations:

$$z \frac{\partial \theta}{\partial z} \rightarrow \frac{\delta \theta}{\delta \ln z} \quad (3-3)$$

$$z \frac{\partial u}{\partial z} \rightarrow \frac{\delta u}{\delta \ln z} \quad (3-4)$$

he defined his "quasi-local" Richardson number as:

$$Ri(z_{1,2}) = 2gz_{1,2}(\theta_2 - \theta_1)\ln(n)/T_2(u_2 - u_1)^2 \quad (3-5)$$

where  $z_{1,2} = (z_1 z_2)^{1/2}$  is the geometric mean height<sup>1</sup>,  $T_2 \approx 1/2(T_1 + T_2)$

---

<sup>1</sup>The geometric mean is used because the logarithm of the geometric mean is the arithmetic mean of the logarithms of the individual heights.

is approximately the mean temperature for the layer, and where  
 $n = z_2/z_1$ .

The simplest formulation of Equation 3-5 is given by Webb (1965). If  $Q$ ,  $N$  and  $Ri$  are defined as:

$$Q = (\theta_2 - \theta_1) / (u_2 - u_1)^2 \quad (3-6)$$

$$N = 9.81 z_{1,2} \ln(z_2/z_1) / \Theta \quad (3-7)$$

then:  $Ri(z_{1,2}) = NQ \quad (3-8)$

Except for variously approximating  $(\theta_2 - \theta_1)$  by  $(T_2 - T_1)$  or  $\Theta$  by  $\bar{T}$  for the layer, this method has been used by such investigators as: Webb (1970), Fichtl and McVehil (1970), Hanna and Panofsky (1969), and Blackadar et al. (1969).

Hanna and Panofsky (1969) have also suggested a method for computing the Richardson number between  $z_0$  and the first anemometer height:

$$Ri(z_0, z_1) = (g/\bar{T}) \left[ (T_1 - T_0) + \Gamma z_1 \right] / (u_1 - u_0)^2 \quad (3-9)$$

$$\left[ (z_1 - z_0)^{\frac{1}{2}} \ln(z_1/z_0) \right]$$

where  $\bar{T}$  is the mean temperature in the layer  $(z_0, z_1)$ ,  $T_0$  is the temperature at  $z_0$ ,  $z_1 \approx (z_1 - z_0)$ ,  $u_0 \equiv 0$ , and  $z_0$  is estimated from a visual inspection of the site itself.

A similar method was developed by Peterson (1974):

$$Ri(z_1) = (g/\Theta)z_1 \left[ \ln(z_1/z_0)^2/(u_1)^2 \right] \frac{\partial \theta}{\partial \ln z} \quad (3-10)$$

where  $\frac{\partial \theta}{\partial \ln z}$  is the slope of the least squares fit to the potential temperature profile in the lowest four tower levels,  $\Theta$  is assumed to be a constant 280°K,  $z_1$  is the height of the first anemometer. At Risø  $z_1$  was 7 m and  $z_1/z_0$  was assumed to be 100. Peterson argued that this departure from the standard method (Equation 3-8) was necessary lest the profile selection be biased in favor of large wind shear in the  $z_1$ - $z_2$  layer resulting in too large an estimate for  $z_0$ .

Following Peterson (1974a), the Richardson number for this study was computed from:

$$Ri(z_0, z_1) = (g/\Theta)(z_1 z_0)^{1/2} \left\{ \left[ \ln(z_1/z_0) \right]^2 / (u_1)^2 \right\} \frac{\partial \theta}{\partial \ln z} \quad (3-11)$$

where  $\Theta$ , the mean potential temperature for the layer ( $z_0, z_1$ ), was estimated by the potential temperature at 2 m;  $z_1$  is the 7 m height; and  $z_0$  is estimated to be 10 cm. This 10 cm estimate is the average of the roughness lengths found by Panofsky and Petersen (1972) in their analysis of the Risø data. The geometric mean for the layer (0.1 m, 7 m) is 0.84 m.

It is more precise to use the geometric mean because, as Paulson (1970) has shown, the following equation holds for any profile variable, F:

$$\frac{\partial F}{\partial z} \Big|_{(z_1 z_2)^{\frac{1}{2}}} \approx \frac{F_2 - F_1}{(z_1 z_2)^{\frac{1}{2}}} \ln(z_1/z_2) \quad (3-12)$$

This expression is rigorous for logarithmic profiles and "for  $F \propto z^{-1/3}$  with observation heights of 0.5 and 16 m (Kerang data), the error is 6%." If in addition  $z_2 = \sqrt{2}z_1$ , then the error involved in approximating the gradients at the geometric mean height with this finite difference scheme is insignificant (Dyer, 1971).

As in previous studies, the effects of water vapor have been assumed to be negligible. This buoyancy effect is known to be important over the ocean, in which case the lapse rate of virtual potential temperature is incorporated in the Richardson number via the transformation:

$$\frac{1}{\Theta} \frac{\partial \theta}{\partial z} \rightarrow \frac{1}{\Theta} \left[ \frac{\partial \theta}{\partial z} \right]_{\text{mod}} \quad (3-13)$$

where:

$$\frac{1}{\Theta} \left[ \frac{\partial \theta}{\partial z} \right]_{\text{mod}} = \frac{1}{\Theta} \frac{\partial \theta}{\partial z} + 0.61 \frac{\partial q}{\partial z} \quad (3-14)$$

Webb (1965). Over land Morgan et al. (1971), in their analysis of the Davis data were able to use the virtual temperature in the computation of the Richardson number; however, such precision is not possible in an analysis of the Risø data.

For neutral stability the Richardson number is identically zero; however, in practical applications it is necessary to assign a finite

interval to this critical value. Without explaining the rationale behind their choice, previous investigators such as Panofsky and Petersen (1972) have used  $\pm 0.005$  to define the limits of the neutral case when the Richardson number is computed between 7 m and 23 m.<sup>2</sup> Hanna and Panofsky (1970) and Deacon (1953) have shown that a linear extrapolation of a Richardson number gives an acceptable approximation; therefore, in this study, the limits of  $\pm 0.005$  were scaled down to  $\pm 0.00035$ .

---

<sup>2</sup>Webb (1970) used  $\pm 0.006$  for a Ri evaluated at a geometric mean height of 1.6 and 2.0 m. Oliver (1971) used  $\pm 0.003$  at a geometric mean height of 20.5 m.

#### IV. TEST OF THE METHOD OF SELECTING NEUTRAL PROFILES AT A HOMOGENEOUS SITE

In 1967 the Wangara expedition to Hay, N.S.W., Australia, resulted in the acquisition of high quality micrometeorological data for the description of the PBL. The Hay area was generally flat and covered with low vegetation. Station Number 5 at Hay was situated near the center of a large field with almost no vegetation except for patches of cotton bush (maximum height 41 cm) about 1 km to the east. The nearest group of large trees was along the Murrumbidgee River 5 km south of the site.

Wind profiles were measured at 1, 2, 4, 8, and 16 m above the surface. Temperature differences were measured between 1 and 2 and 2 and 4 m. Forty days data were collected. Each hourly observation was a 30 minute hour centered average.

Clarke et al. (1971) carefully selected 42 neutral and near-neutral profiles primarily on the basis of the temperature gradient. If the upper portion of the profile departed from linear, then  $z_0$  was computed from only the lower portion of the profile. In either case his  $z_0$  was found from fitting Equation 1-1 to the data; the resulting average  $z_0$  was  $0.12 \pm 0.01$  cm (the correct procedure is to average the values of the  $\ln(z_0)$ ). No significant dependence of  $z_0$  on wind direction was found.

For this study 36 of Clarke's neutral profiles were reanalyzed by extrapolating from the 8-16 m layer to compute  $\ln(z_0)$ . Six of Clarke's neutral profiles were excluded -- three because they were centered on the half-hour and not in the published data, and the other three for the reasons cited below. The results are presented in Table 2.

Two methods for selecting neutral profiles were tested. Method I was chosen to be as analogous as possible to the method used both in this study and by Peterson (1974a). Profiles were selected (without reference to wind direction) on the following bases:

1. No temperature or wind data could be missing (this excluded one of the profiles used by Clarke).
2. The 8 m wind speed had to be greater than 2.5 mps (this excluded two more of the profiles used by Clarke).
3. Wind speed increased with height between 8 and 16 m.
4. For the segment of the profile between 1 and 16 m,  $\partial\theta/\partial\ln z \approx \Delta\theta/\Delta\ln z$  where the finite differences were computed over the 1-4 m layer.
5. The Richardson number was computed from Equation 3-11 with  $z_0$  equal to 1.2 mm and  $\Theta \approx T_{sfc}$ .
6. Neutral cases were accepted if the Richardson number was within  $\pm 0.00035$  of zero. These were the same limits that were used on the  $Ris\phi$  data for the 0-7 m layer.

7. The  $\ln(z_0)$  was computed by extrapolating from the 8-16 m layer.

Method II was the same as Method I except that the Richardson number was computed from Equation 3-12 adapted to the 8-16 m layer (geometric mean height of 11.3 m) with a tolerance on the neutral Richardson number of  $\pm 0.0065$ . In using the wind shear in the 8-16 m layer, Method II approximates the method of Panofsky and Petersen which used Equation 3-8.

Table 2 compares these three methods of selecting neutral profiles for the computation of  $z_0$ . Method I missed 19 of the 36 neutral profiles selected by Clarke et al. (1971) and Method II missed 33. Clarke's mean profile (for the 36 profiles discussed here) resulted in a  $z_0$  very close to the previously published value. The values of the  $\ln(z_0)$  extrapolated from the 8-16 m level were well behaved. The dispersion was fairly small, the cumulative normal distribution was nearly linear, and the data were not significantly skewed. However, the departure of the kurtosis from normality was significant at the 90% level (two sided Geary's test).

In general Methods I and II agree to within one order of magnitude; however, Method I agrees best with Clarke's results. The differences between Methods I and II are as follows:

1. The  $z_0$  computed for the Method I mean profile is in good agreement with the results published by Clarke et al. while the  $z_0$  from Method II is not.

Table 2. Comparison of the Wangara neutral profiles selected by various methods.

	Clark	Method I	Method II
No. of profiles	36	35	6
Mean 4 m wind (mps)	6.43	6.18	5.14
Mean 8 m wind (mps)	7.06	6.75	5.60
Mean 16 m wind (mps)	7.61	7.27	6.08
Coefficient of linear regression	0.9992	0.9997	0.9999
$z_0$ from mean profile (cm)	0.116	0.10	0.25
Average $z_0$ (cm) from individual profiles	0.35	0.55	1.24
Std dev of $z_0$ from individual profiles	0.88	0.26	1.93
Average $\ln(z_0)$ ( $z_0$ in cm)	-7.21 (0.074)	-7.48 (0.056)	-6.31 (0.18)
Std dev of $\ln(z_0)$	1.90	2.71	2.94
Range of $\ln(z_0)$	7.86	14.40	7.34
Skewness of $\ln(z_0)$	0.02	-1.15	-0.40
Kurtosis of $\ln(z_0)$	2.27	5.80	1.57

2. Method II selects far fewer cases than either of the others although Method II cases were a subset of those from Method I.
3. Method I selects higher wind speed profiles than Method II.
4. Although both methods give mean profiles which appear to be straight lines when plotted on semi-logarithmic graph paper, the regression coefficient shows that the mean profile from Method II is slightly straighter.
5. For Method I the dispersion in the data was smallest and the average  $\ln(z_0)$  was very close to that of Clarke.
6. Method II results in slightly larger roughness lengths supporting Peterson's (1974a) argument against this method, but both methods agree to within one order of magnitude.

## V. DATA AND SITE DESCRIPTION

The Research Establishment Risø of the Danish Atomic Energy Commission is located on the Risø peninsula 6 km north of Roskilde, Denmark (Figure 5). This tongue of land consists of low rolling hills bounded by the irregular coastline of Roskilde Fjord. The largest orographic feature within 1000 m of the tower is a 10 m bluff on the Veddelev peninsula about 800 m southwestwards (Figure 6).

The 123 m meteorological tower is located about 100 m northwards from the closest shore on a low, smooth hill 6.5 m MSL cluttered with buildings and trees. The instruments are mounted on booms pointing southwest. Ambient air temperature measurements are taken at eight heights above the tower's base: 2 m, 7 m, 23 m, 39 m, 56 m, 72 m, 96 m, and 125 m; the wind speeds are measured at seven heights starting at the 7 m level; wind direction measurements are taken at 7 m, 56 m, and 125 m; and lastly, moisture is measured at 2 m and 125 m. The topmost instruments are mounted directly above the tower. Panofsky and Petersen (1972) have published a complete description of the Risø tower, its configuration and instrumentation.

Except for occasional instrument malfunctions, continuous ten year records (3/58 - 12/67) exist on nine channel magnetic tape in Burroughs B6500 hexadecimal format. These data were transcribed

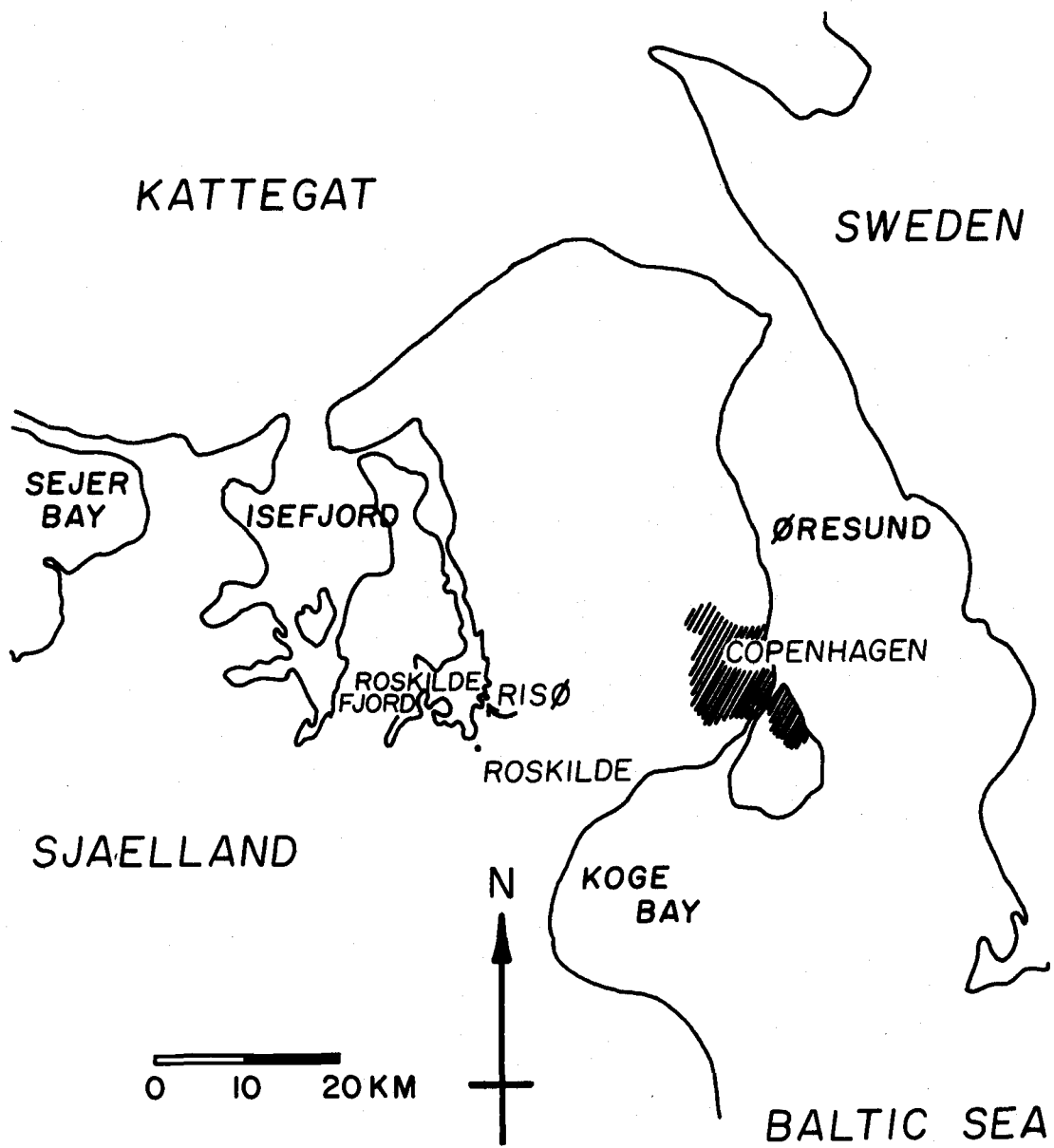


Figure 5. Map of eastern Denmark.

by Risø personnel from strip charts and consist of ten minute averages centered on each hour. The wind directions were measured to the nearest ten degrees; the wind speed was recorded to the nearest 0.5 mps from 1958 through 1963 and to the nearest 0.1 mps from then on. The temperature data are estimated to be accurate to within  $\pm 0.1^{\circ}\text{C}$ ; however, Peterson (1974) detected a systematic error in the temperature measurements of  $0.4^{\circ}\text{C}$  per 100 m for the years 1963 through 1967. The necessary temperature correction was included in the data reduction for this study.

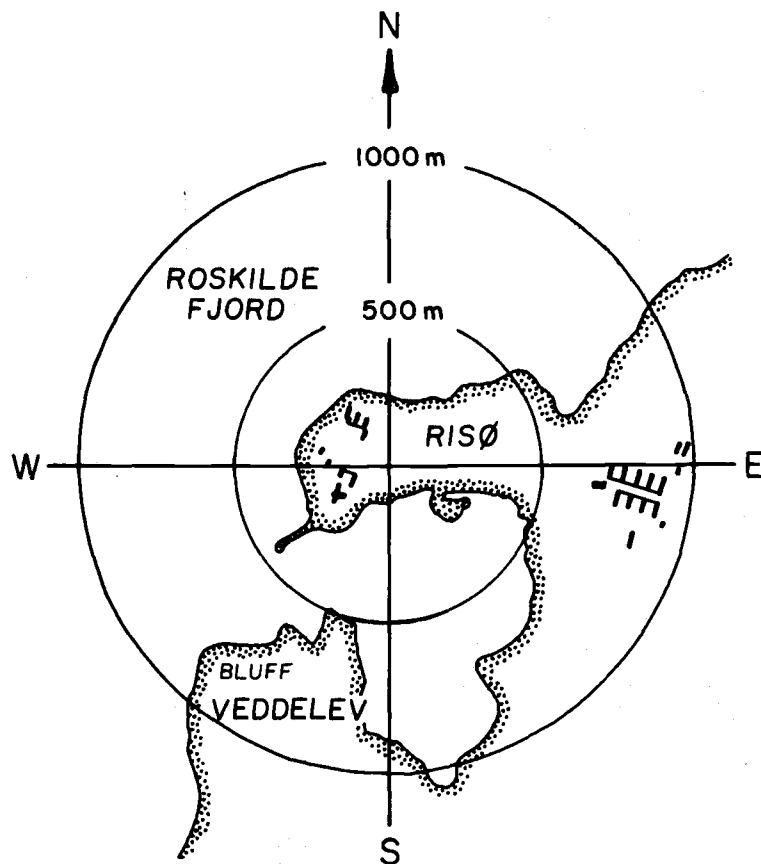


Figure 6. Map of Risø and vicinity.

## VI. REDUCTION OF THE OBSERVATIONS

Panofsky and Petersen (1972) separated the data into 11 wind direction groups (Table 3). Observations were excluded under these conditions:

1. If any wind direction, speed, or temperature was missing.
2. If the 7 m wind speed was less than 2.5 mps.
3. If no two wind directions fell within the range of wind directions specified for a particular group.

Each profile was then averaged over three consecutive hours in order to smooth the data. Within each group the profiles were segregated into five Richardson number categories using Equations 3-6 through 3-8. This scheme of analysis was also used by Petersen and Taylor (1973).

Peterson (1974a and 1974b) separated the data into several classes (Table 3). He excluded observations under the following conditions:

1. If any wind speed or temperature was missing.
2. If the 56 m wind direction was missing.
3. If the 7 m wind speed was less than 2.5 mps.
4. If the wind speed did not increase to at least 39 m.
5. If the wind speed decreased with height above 39 m.
6. If the temperature changed by more than  $\pm 0.5$  C between layers.

Table 3. Comparison of the values of  $z_0$  found by previous investigators at Risø.

Class	Group	Direction deg*	Distance in m to: water : far shore		Panofsky and Petersen		Petersen and Taylor		Peterson			
					Number of profiles averaged	$z_0$ in cm	Number of profiles averaged	$z_0$ in cm	Class	Direction Deg	Number of profiles averaged	$z_0$ in cm
A	1	81-101	---	---	49	7	---	---				
	2	101-121	---	---	51	1	---	---				
	3	121-141	300	600	77	5	77	5				
	4	141-161	100**	700**	42	6	42	6	A	85-225	364	0.03
B	5	161-191	100	900	53	10	53	10				
	6	191-211	200	600	77	2	78	2	B	185-225	142	0.053
	7	211-241	300	700	255	12	286	13				
---	8	241-271	300	2500	505	30	---	---	C	225-245	113	2.3
C	9	271-301	300	6500	458	22	605	22	D	245-265	161	7.6
	10	301-331	280	5500	185	28	256	28	E	225-005	455	5.5
	11	331-001	280	4500	68	5	79	5				

\* Corrected for the 4° error found by Peterson (1974a)

\*\* Islands in the water

7. If both the average lapse rate in the lowest 39 meters and the overall lapse rate were not within  $\pm 0.2$  C per 100 m of the adiabatic lapse rate.

Neutral profiles were then selected by Richardson number using an equivalent form of Equation 3-10. Peterson did not average the profiles over three consecutive hours because the boundary layer is rarely stationary over such a long period of time.

For this study of the variation in the surface roughness lengths, it is only necessary to characterize the profiles on the basis of the lowest 39 meters in order to insure the accurate computation of  $z_0$ . This approach minimizes the complications caused by the upstream variation of the roughness, the change of stress with height, and the buoyancy effects. The data were separated into eight wind direction groups using the 7 m wind direction (Table 4).

These groups were selected in a way which roughly balances the need for large numbers of neutral cases against the irregularity of the terrain and the desire to have some basis for comparison with the previous investigations (Figure 7).

At Risø the instruments are on booms extending outward from the tower towards the southwest. Dabberdt (1968) has shown that decreases of wind speed of up to 35% are possible downwind of a triangular tower with a perimeter three times as long as the perimeter of the Risø tower and that the velocity defect area extends

Table 4. Comparison of the values of  $z_0$  (from ten year mean profiles) found by previous investigators and those of this study.

Sector Deg	Number of Neutral Profiles	Group	Number of Neutral Profiles	Average distance in m to Near shore*	This study**		Peterson		Panofsky and Petersen
					$z_0$ in cm	$z_0$ in cm	$z_0$ in cm	$z_0$ in cm	$z_0$ in cm
85-95	144	1	614	---	0.66		---		4
95-105	157					↑		↑	
105-115	162								
115-125	151								
125-135	177	2	527	235	0.002		---		5.3
135-145	224								
145-155	126					0.04		0.034	
155-165	102	3	322	100	0.003		---		9
165-175	63								
175-185	57								
185-195	100								
195-205	134	4	502	235	0.018	↓	0.05	↓	5.3
205-215	189								
215-225	179								
225-235	235	5	972	300	0.77	0.77	2.3	2.3	12
235-245	737								
245-255	252	6	1293	300	7.53	↑	7.6	↑	28
255-265	170								
265-275	446								
275-285	425								
285-295	324	7	713	290	10.06	7.13	---	6.3	25
295-305	179								
305-315	130								
315-325	80								
325-335	74	8	350	280	2.14	↓	---	↓	12
335-345	92								
345-355	82								
355-005	102								

\* Estimated from Panofsky and Peterson (1972)

\*\* Mean profile was averaged over all speed categories

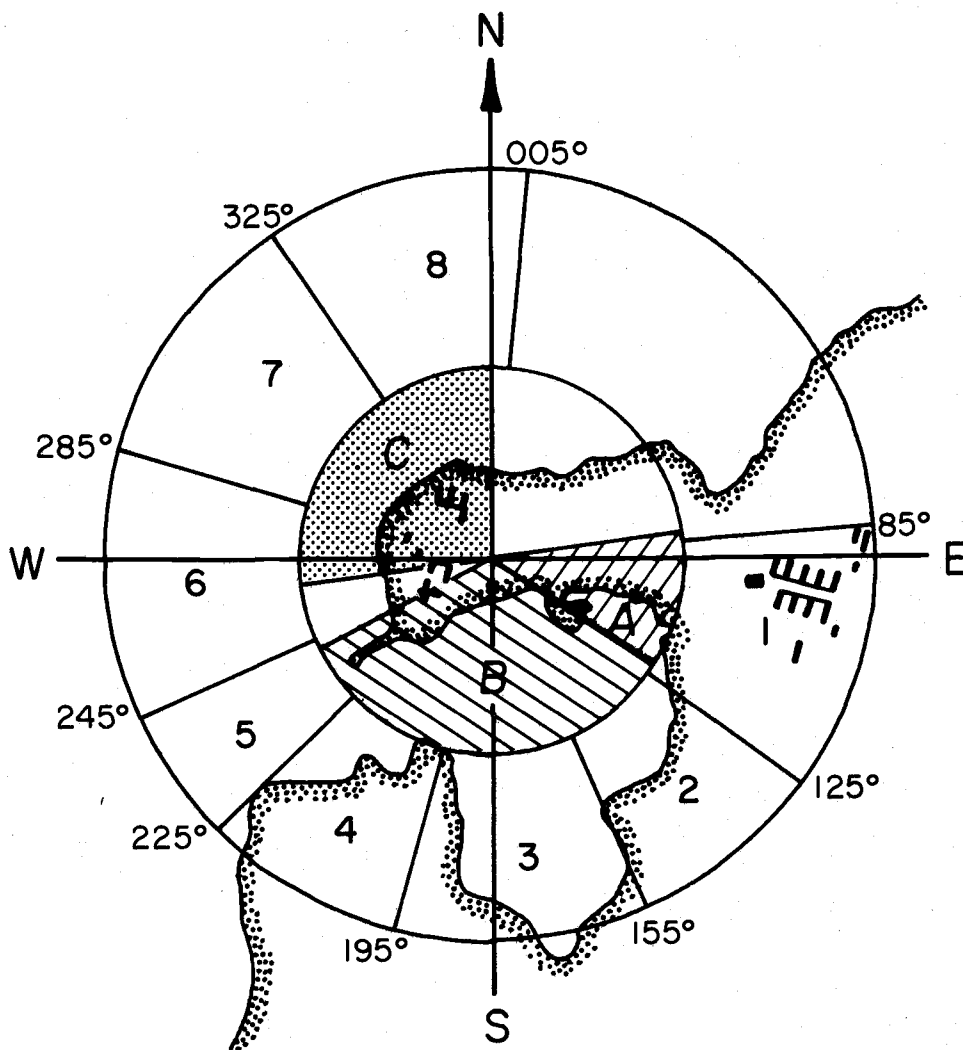


Figure 7. Map of Risø area showing Panofsky and Petersen's Classes A, B, and C and the direction groups 1-8 of this study.

through a  $60^\circ$  sector. To avoid these complications, profiles were excluded if the 7 m direction was between  $005^\circ$  and  $085^\circ$ . Observations were also excluded if any of the following conditions occurred:

1. If any temperature or wind speed was missing between 2 m and 39 m.
2. If the 7 m wind direction was missing.
3. If the 7 m wind speed was less than 2.5 mps.
4. If the wind speed did not increase with height to at least 39 m.
5. If the corrected temperatures between 2 m and 39 m varied by more than  $\pm 0.5$  C between levels.

This last condition was first imposed by Peterson (1974a) to help filter out erroneous temperature measurements since a careful examination of the Risø data shows that there is normally little variation in the temperature between layers. Within each direction group the profiles were separated into stable, neutral, and unstable categories using Equation 3-11 with the lapse rate of potential temperature computed from the slope of the least squares fit to the semi-logarithmic plot of the lowest four potential temperatures. Ri Category 1 is the stable case, Ri Category 2 neutral, and Ri Category 3 unstable. Within each stability category, the profiles were further segregated into three wind speed categories according to the 7 m wind speed. Category 1 wind speed is from 2.5 mps to 7.5 mps; Category 2 is from 7.5 mps to 12.5 mps; and Category 3 is for 12.5 mps and above.

## VII. TEN YEAR MEAN PROFILES

Figure 8 shows the ten year mean neutral profiles averaged over all speed categories. These profiles are all distinctly concave down instead of being linear as predicted from the theory for flow over homogeneous terrain (Equation 1-1). The standard deviations of the wind speeds are rather large (from about 0.5 to 1.7 mps), and except for the Group 5 profile, they can all be straightened well within the 99% confidence intervals for the mean wind speeds. Unfortunately, previous investigators did not publish anything except mean wind speeds, so it is impossible to compare distributions.

Curvature of a profile concave down normally indicates a stable case (Figure 9). However, such curvature was expected after the results of Peterson (1974a). Figures 10 and 11 show the comparison between the mean profiles selected by the method of Peterson and those selected by the method of Panofsky and Petersen. As previously noticed by Peterson, the Panofsky and Petersen method selects profiles biased in favor of higher than average roughness lengths since it selects for high 23 m wind speed and low 7 m wind speed. This results from making the selection based on the following Richardson number:

$$Ri = \frac{(\text{const})}{\Theta} (\theta_{23} - \theta_7) / (u_{23} - u_7)^2 \quad (7-1)$$

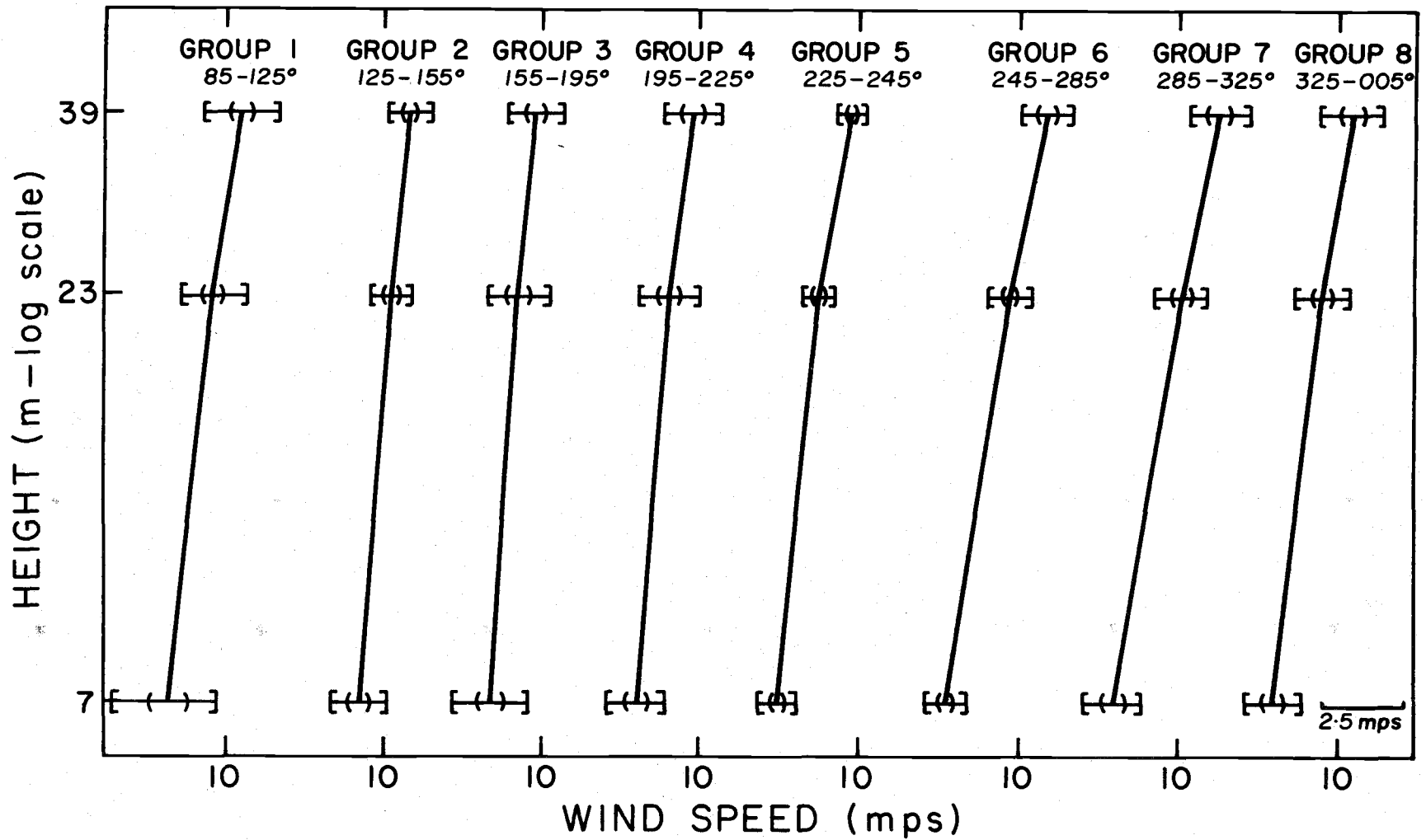


Figure 8. Ten year mean profiles averaged over all wind speeds. Horizontal bars with brackets indicate the standard deviation. Horizontal bars with parentheses indicate the 99% confidence intervals for the mean wind speeds.

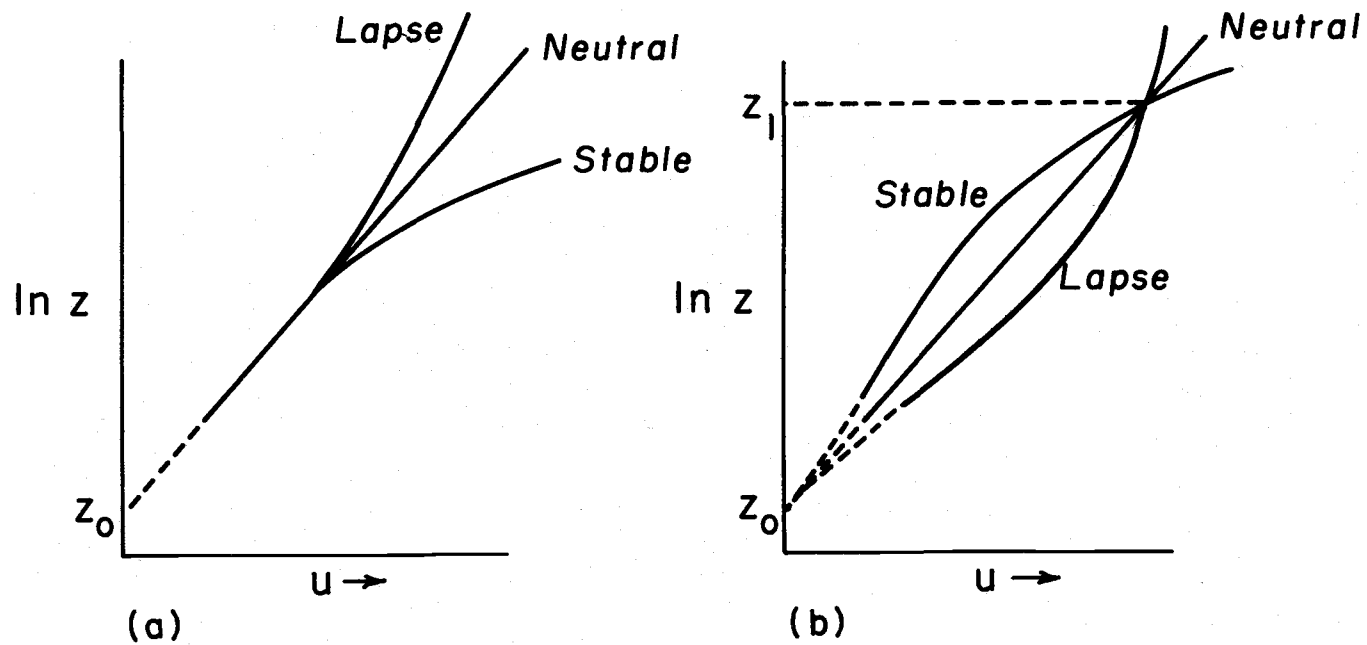


Figure 9. Form of the wind profile over a surface of roughness  $z_0$ , in lapse, neutral, and stable conditions, plotted against a logarithmic height scale. (a) illustrates three cases having the same value of  $u_*$ , so that the three curves have the same slope at small heights. (b) illustrates three cases with the same wind speed at some reference height  $z_1$ . After Webb (1965).

which has the square of the 7-23 m wind shear in the denominator.

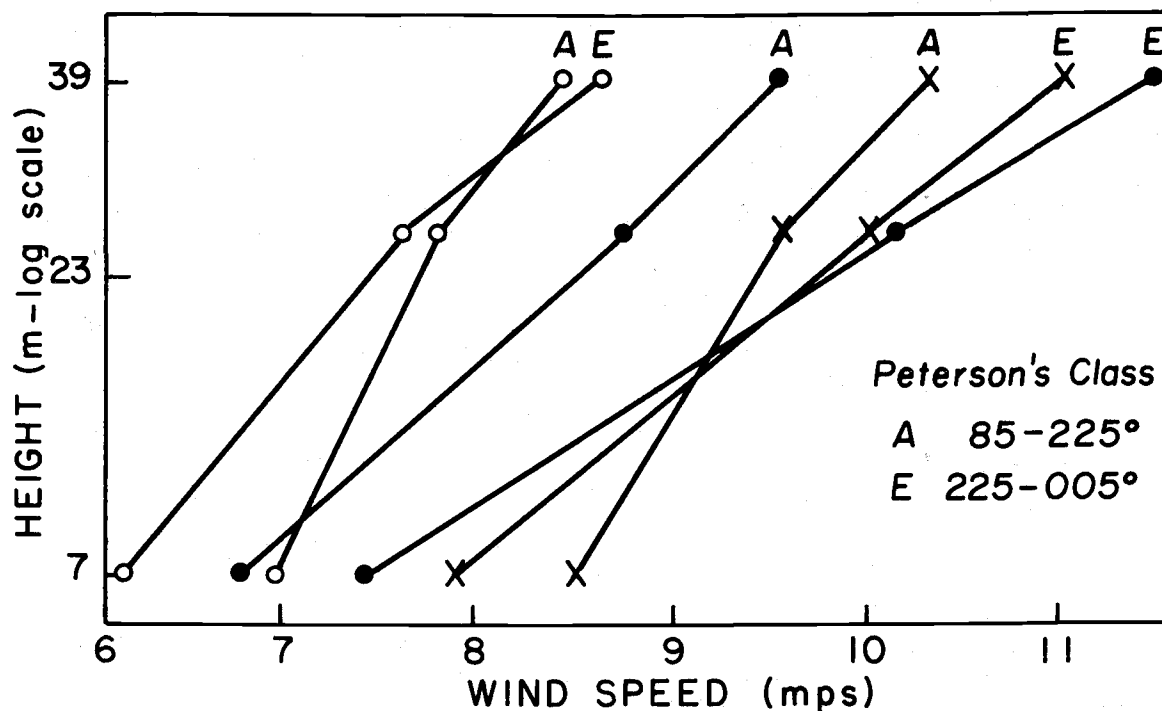


Figure 10. Ten year mean profiles selected by Peterson's method (open circles), Panofsky and Petersen's method (closed circles) (Both after Peterson, 1974a), and current study (crosses).

In this study the Richardson number was computed as follows:

$$Ri = \frac{(\text{const})}{\Theta} \frac{\partial \theta}{\partial \ln z} (u_7 - u_0)^{-2} \quad (7-2)$$

If computation of the Richardson number necessarily requires bias in favor of large wind shear in some layer, then it is best to have the large shear in the  $z_0$ -7 m layer as is illustrated by the following simplified example of flow over a smooth fjord moving onto a rougher coast (Figure 12). This figure depicts neutrally stratified flow over

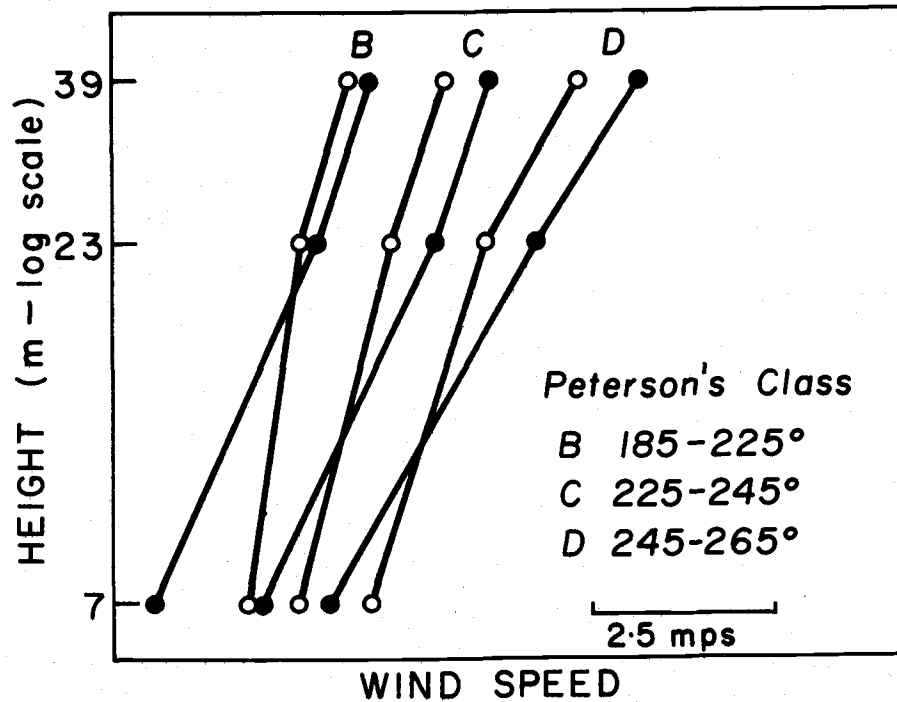


Figure 11. Comparison (by superposition) of the curvature of the ten year mean profiles selected by Peterson's method (open circles) and by Panofsky and Petersen's method (closed circles). (Both after Peterson, 1974a).

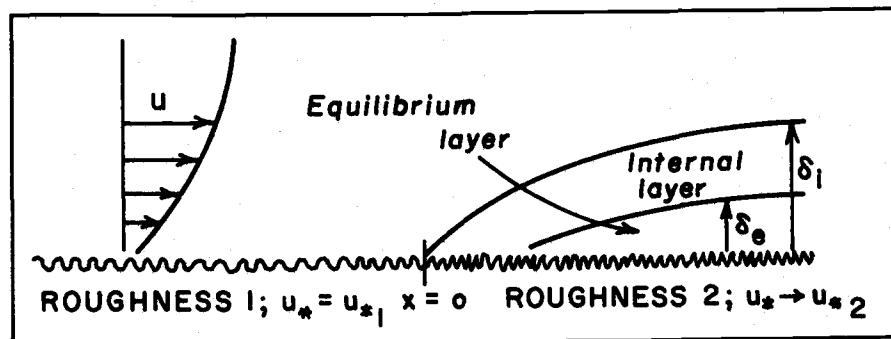


Figure 12. Schematic of the simplest inhomogeneity problem - a singular one-dimensional change in surface roughness. (After Wyngaard, 1973).

the smooth surface of the fjord encountering the coast resulting in a step change in surface roughness at  $x = 0$ . For fully turbulent flow with an eddy length scale of  $l$ , the structure of the turbulence responds to this change with a characteristic time scale of  $l/u$ . This results in the development of an internal layer within which the flow is still adjusting to the change in surface roughness. Further inland and below the internal layer is an equilibrium layer within which the flow is once again in equilibrium with the surface.

The height of the equilibrium layer can be estimated by:

$$\delta_e = 0.01x \quad (7-3)$$

and the height of the internal layer by:

$$\delta_i = 0.75x^{0.8} \quad (7-4)$$

Equation 7-3 agrees both with the laboratory data of Antonia and Luxton (1971) and the model calculations of Peterson (1969). Although Equation 7-4 is from the simple model of Elliott (1958) it is substantially in agreement with the later, more sophisticated models (e. g., Peterson, 1969). The Risø tower is from 100 to 300 m from the shore (Table 3); therefore, the equilibrium layer should be about 1 to 3 meters thick while the height of the internal layer should vary between 25 and 55 meters.

In view of the terrain complication it should be best to compute the Richardson numbers from Equation 7-2 so that no data used in the computation will come from the layer dominated by the roughness, humidity flux and heat flux of the fjord.

Surface roughness lengths were computed from the ten year mean profiles (Figure 8) using the following three possible methods: (1) extrapolating from the 23-39 m layer, (2) extrapolating from the 7-23 m layer, and (3) using a least squares fit to the 7, 23, and 39 m winds. The results are presented in Table 5.

The roughness lengths computed from the 23-39 m layer are rather large and would be roughly comparable to the results of Panofsky and Petersen (1972) were it not that the values of  $z_0$  for Groups 2 and 3 are an order of magnitude too low for consistency.

The least squares fit gives intermediate values of  $z_0$ , but there is no reason to expect that the results will be improved by averaging data from different types of boundary layers. Only in Group 5 is the result interesting; here the least squares fit gives good agreement with Peterson's  $z_0$ .

Both the 7 m and the 23 m levels should be within the internal layer where the flow is at least partially influenced by the surface characteristics of the peninsula. The ten year mean surface roughness lengths for the two broad sectors are in good agreement with those computed by Peterson (1974a). The direction groups with the largest

Table 5. Comparison of roughness lengths computed from the ten year mean profiles by (1) extrapolating from the 7 and 23 m heights, (2) extrapolating from the 23 and 39 m heights, and (3) fitting a least squares fit to these three heights.

Group	7-23 m	7-23 m	23-39 m	Least Squares	Peterson (1974)	Panofsky & Petersen (1972)*
	$\ln(z_0)$ ( $z_0$ in cm)					
1	-5.03 (0.66)	↑ -7.82 (0.04)	-2.86 (5.70)	-4.37 (1.27)	↑ -7.99 (0.03)	-3.23 (4.0)
2	-10.83 (0.002)		-5.23 (0.54)	-8.72 (0.02)		-2.94 (5.3)
3	-10.41 (0.003)	↓	-5.82 (0.30)	-8.82 (0.02)	↓	-2.41 (9.0)
4	-8.63 (0.02)		-3.30 (3.69)	-6.85 (0.10)		-2.94 (5.3)
5	-4.87 (0.77)	-4.87 (0.77)	-1.78 (16.8)	-3.78 (2.28)	-3.77 (2.30)	-2.12 (12.0)**
6	-2.59 (7.53)	↑	-1.51 (22.0)	-2.31 (9.98)	↑	-1.27 (28.0)
7	-2.30 (10.1)		-2.64 (7.13)	-1.51 (22.0)		-2.10 (12.2)
8	-3.85 (2.14)	↓	-2.31 (9.96)	-3.41 (3.29)	↓	-2.12 (12.0)

\* Estimated for these direction groups

\*\* Peterson (1974b) computed 14.5 cm using Panofsky and Petersen's method

roughness elements (Groups 6, 7, and 8) had the smallest change in the magnitude of  $z_0$  when computed from this layer rather than the 23-39 m layer. This trend was also noted by Slade (1969).

Figures 10 and 13 compare the ten year mean profiles from Groups 1-4, 5, 5-8 (Peterson's Classes A, C, and E). The most significant difference between the results of this study and the Peterson study is the increase in the mean square 7 m wind speed of 49%, 66% and 62%, respectively. This increase is consistent with the limits placed upon the neutral Richardson number in each study. Peterson (1974a) accepted neutral cases when the Richardson number was within  $\pm 0.005$  of zero; however, for this study, the acceptable tolerance was reduced to  $\pm 0.00035$ .

The anomalous behavior of the Group 5 profile is unexplained. This sector is distinguished by a fairly long relatively unobstructed fetch to the near shore and then a long over water fetch (Figure 14).

Figure 14 shows the azimuthal distribution of surface roughness lengths computed from the ten year mean profiles. The pattern is one of high roughness lengths in the sectors dominated by the influence of buildings and the other larger roughness elements on the Risø peninsula but of anomalously low roughness lengths in the sectors with a pronounced double change of terrain.

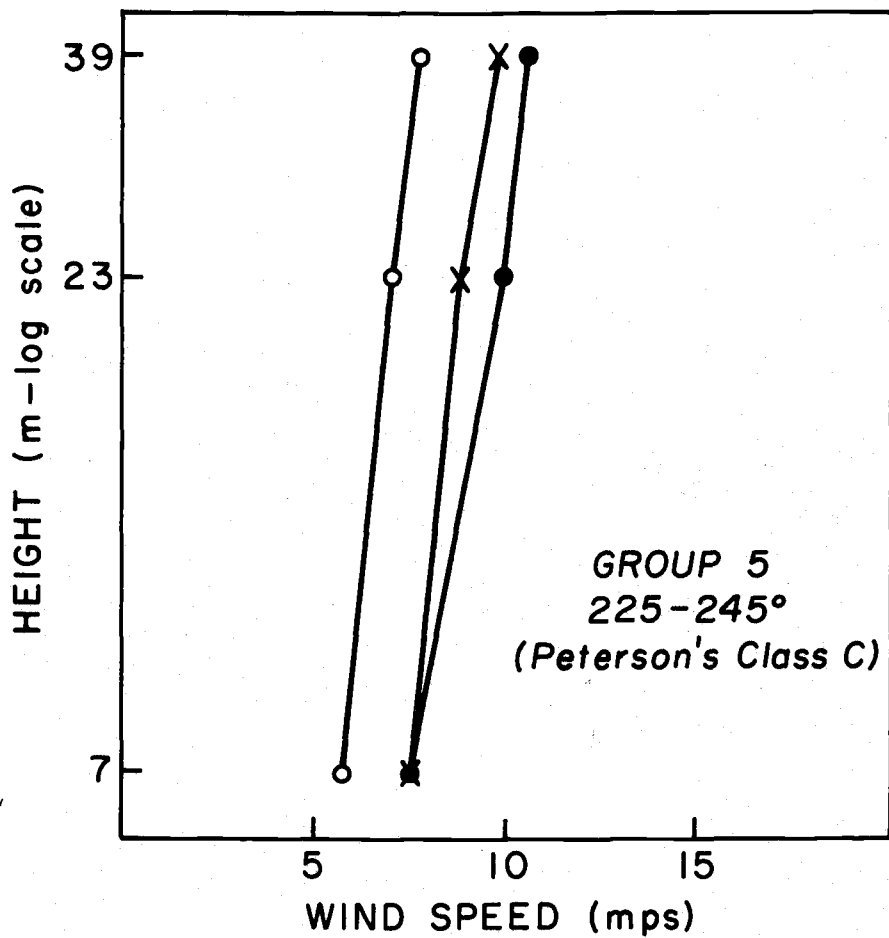


Figure 13. Ten year mean profiles selected by Peterson's method (open circles), Panofsky and Petersen's method (closed circles) (Both after Peterson, 1974b), and by this study (crosses).

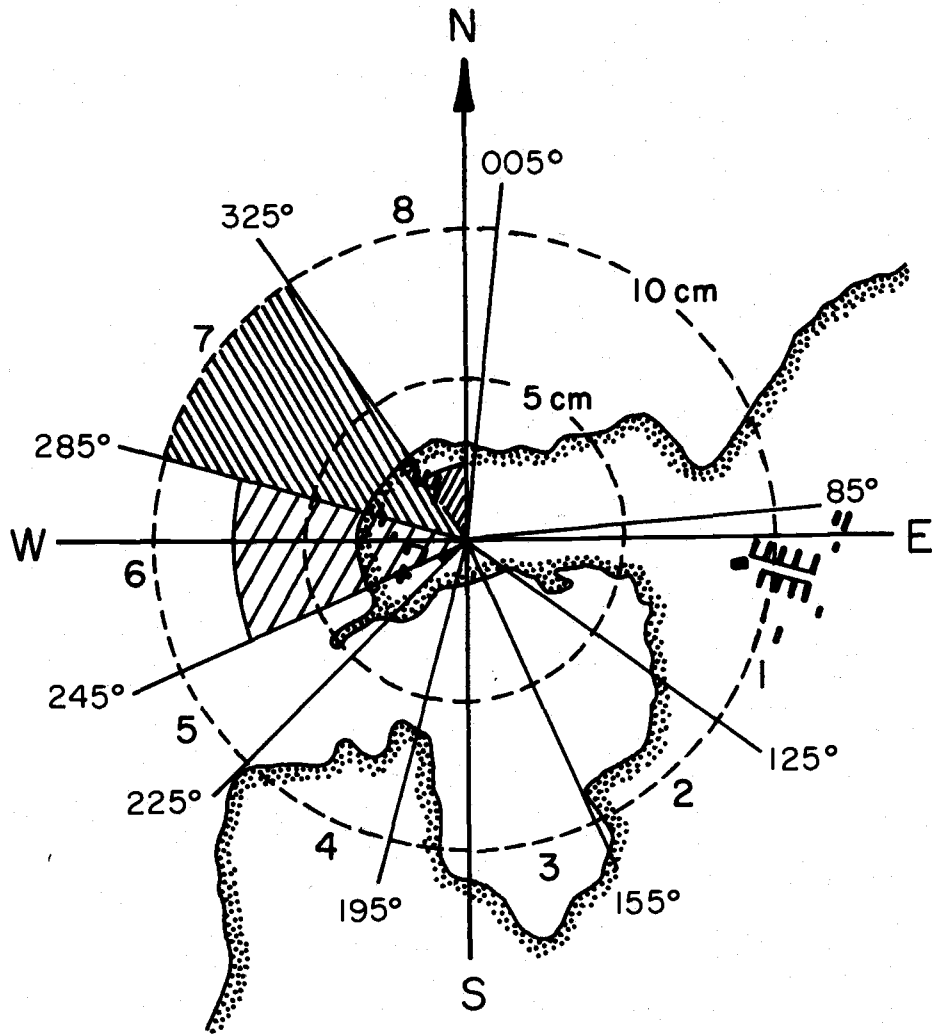


Figure 14. Map of Risø showing the azimuthal distribution of surface roughness lengths. Roughness lengths in Groups 1-4 are so small as to be off scale.

### VIII. ANNUAL AND SEASONAL VARIATION OF THE SURFACE ROUGHNESS LENGTHS

Figures 15 through 22 show the variation in the surface roughness lengths for each group. These  $z_0$  values were computed from the mean annual profiles. Each annual profile is made up of at least two individual neutral profiles. The realization for the Category 3 winds is often broken because of an insufficient number of high speed profiles.

The autocorrelations of the  $\ln(z_0)$  for wind Categories 1 and 2 are plotted in the inserts to Figures 15 through 22. The autocorrelograms all show pronounced periodicities except for those for Groups 6 and 7 which have the closest resemblance to those of purely random and stationary data (Figure B-1(b)). In general, the autocorrelograms suggest that the surface roughness is a periodic function of the long term weather patterns. However, the visual appearance of the autocorrelation functions for short time series can be deceptive and large periodicities can exist even in "white noise."

The realizations themselves are quite remarkable and the results unexpected. The data vary over several orders of magnitude and, in general, the roughness lengths decrease with increasing wind speed. The realizations for Groups 6 and 7 are the best behaved and, from 1961 through 1967, they are the most in keeping with what could have been expected from previous work in this area.

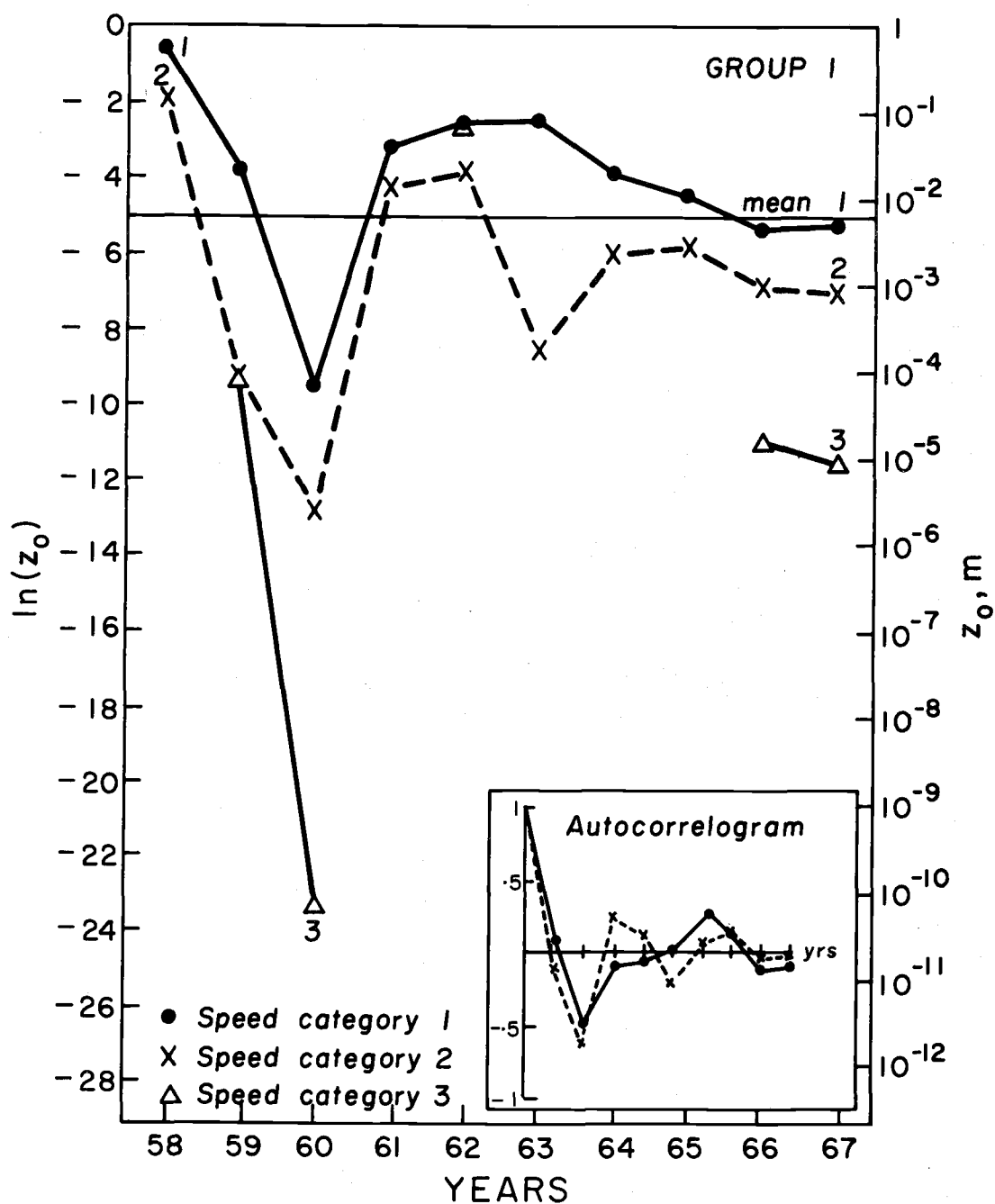


Figure 15. Annual variation of roughness lengths computed from the mean annual neutral profiles. Horizontal line indicates the mean  $z_0$  computed from the ten year mean profiles weighted over all speed categories.

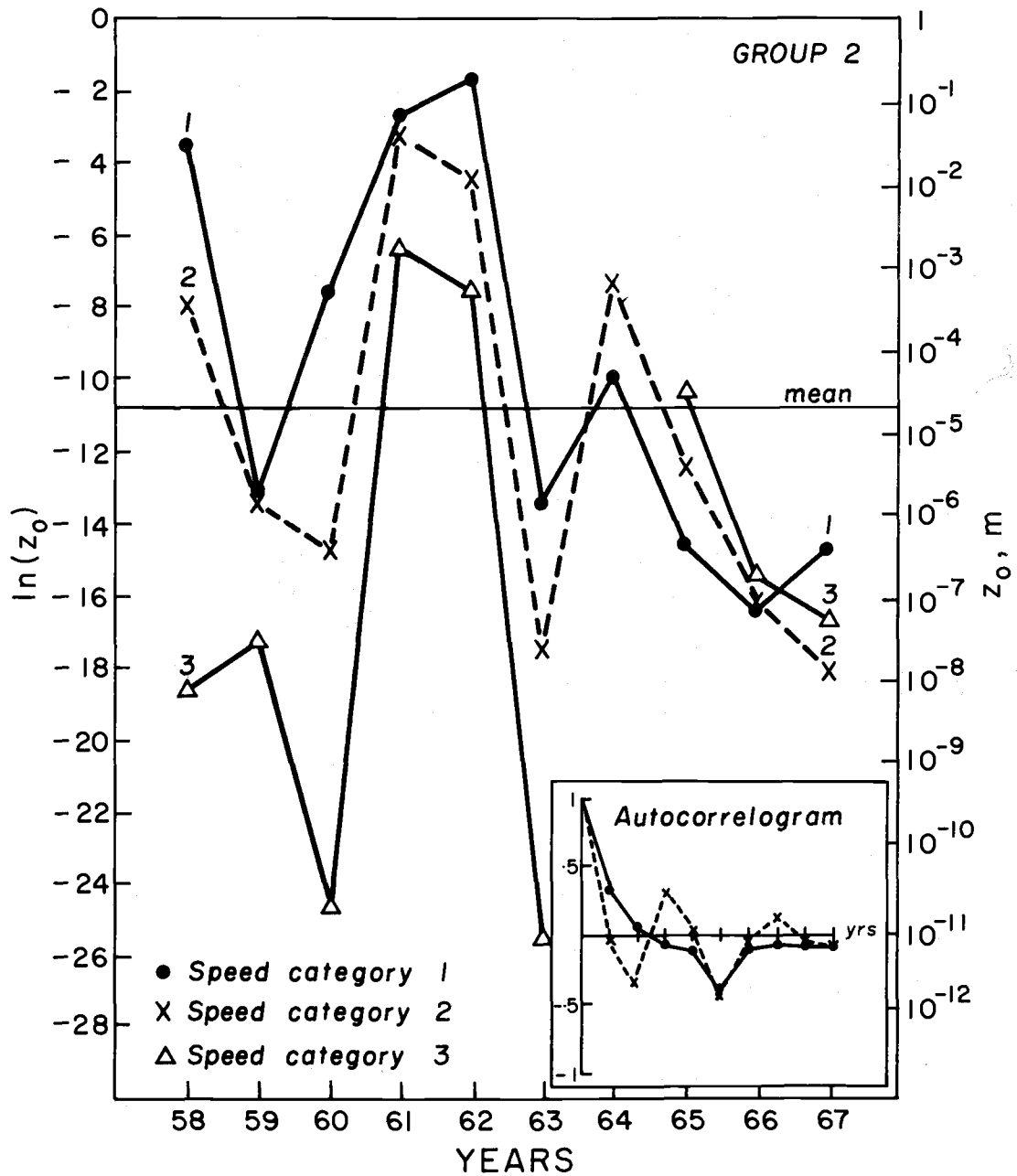


Figure 16. Annual variation of roughness lengths computed from the mean annual neutral profiles. Horizontal line indicates the mean  $z_0$  computed from the ten year mean profiles weighted over all speed categories.

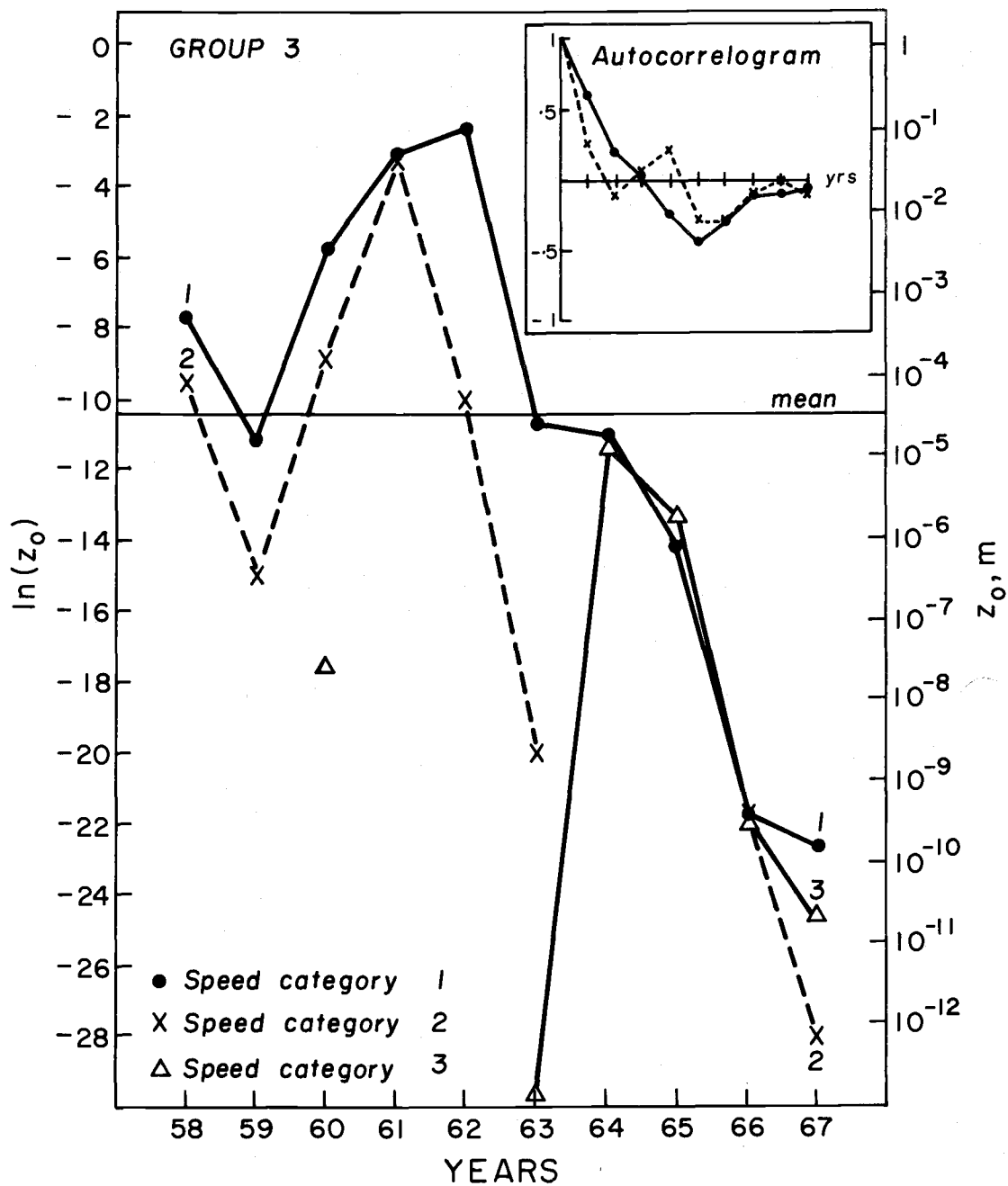


Figure 17. Annual variation of roughness lengths computed from the mean annual neutral profiles. Horizontal line indicates the mean  $z_0$  computed from the ten year mean profiles weighted over all speed categories.

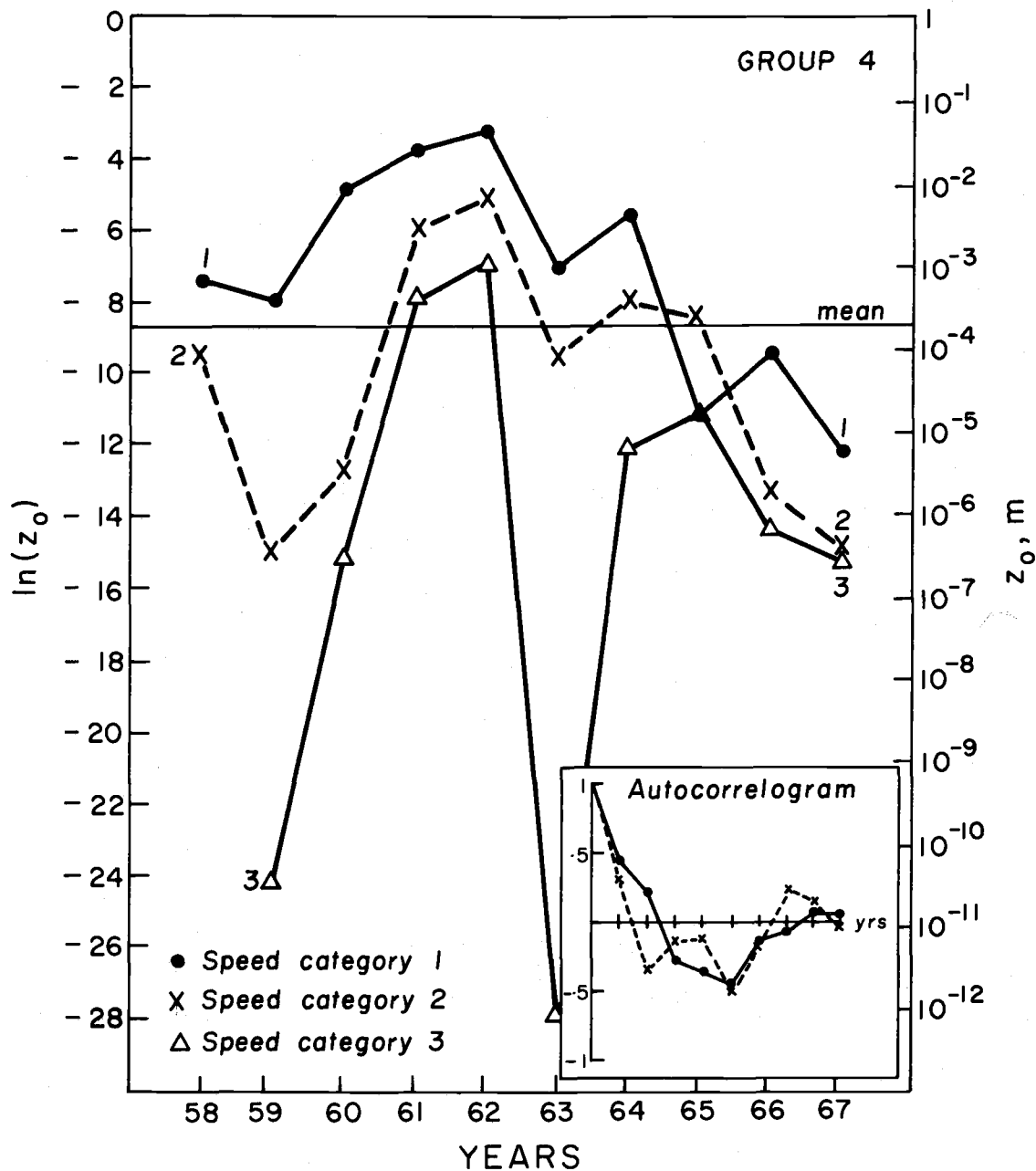


Figure 18. Annual variation of roughness lengths computed from the mean annual neutral profiles. Horizontal line indicates the mean  $z_0$  computed from the ten year mean profiles weighted over all speed categories.

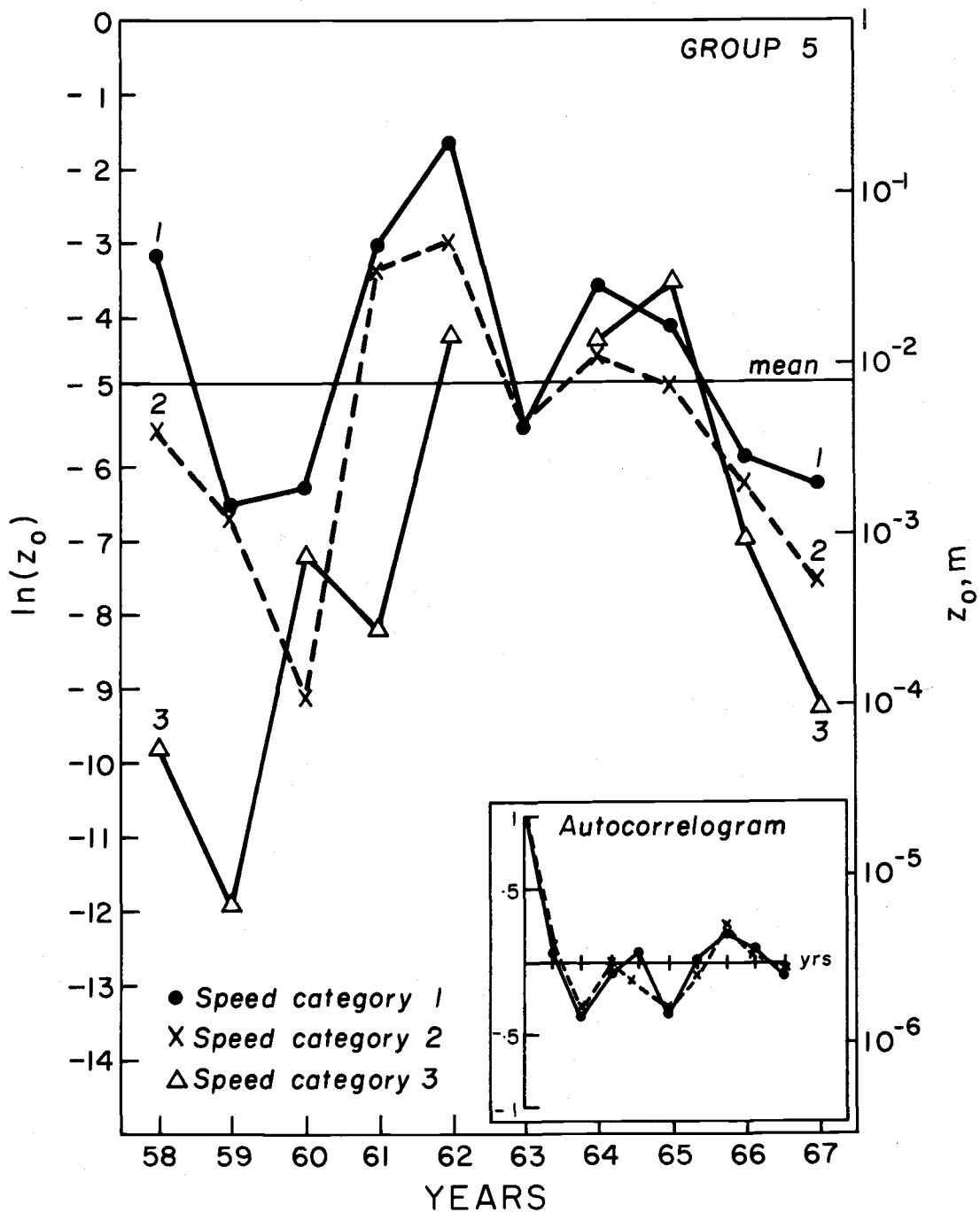


Figure 19. Annual variation of roughness lengths computed from the mean annual neutral profiles. Horizontal line indicates the mean  $z_0$  computed from the ten year mean profiles weighted over all speed categories.

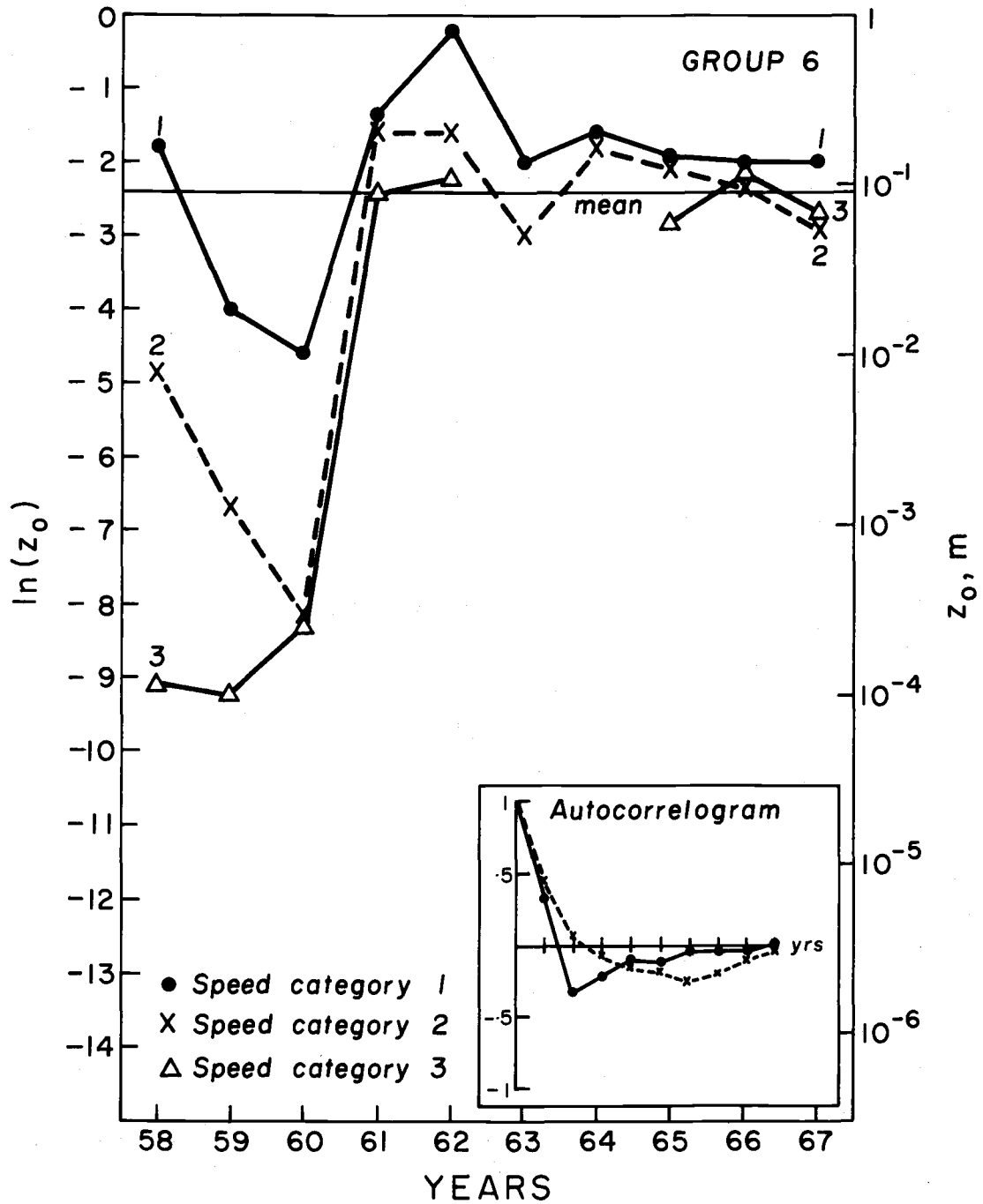


Figure 20. Annual variation of roughness lengths computed from the mean annual neutral profiles. Horizontal line indicates the mean  $z_0$  computed from the ten year mean profiles weighted over all speed categories.

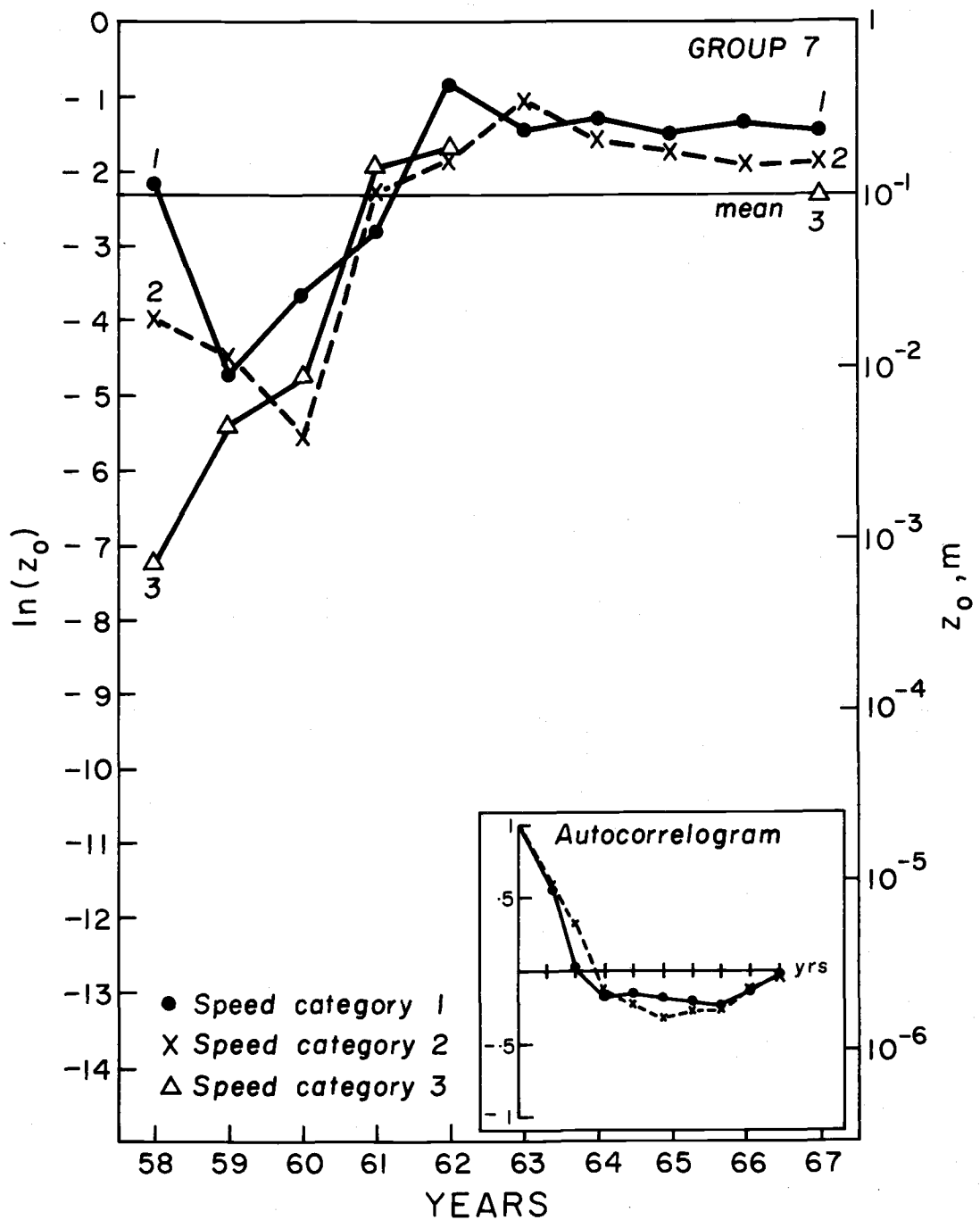


Figure 21. Annual variation of roughness lengths computed from the mean annual neutral profiles. Horizontal line indicates the mean  $z_0$  computed from the ten year mean profiles weighted over all speed categories.

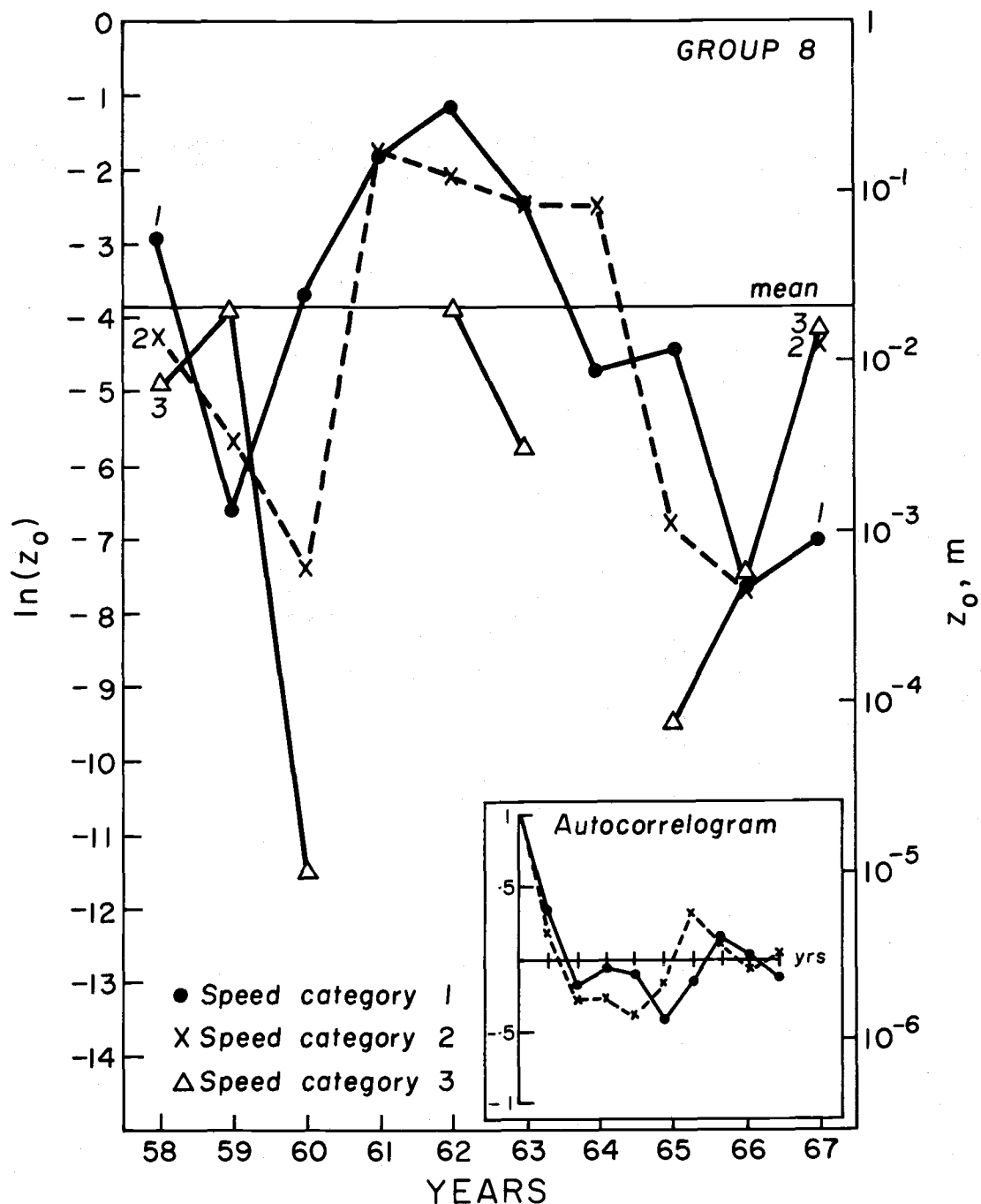


Figure 22. Annual variation of roughness lengths computed from the mean annual neutral profiles. Horizontal line indicates the mean  $z_0$  computed from the ten year mean profiles weighted over all speed categories.

Table 6 summarizes the statistics for this data. There is a consistent trend towards decreased roughness lengths with increased wind speeds except in Group 8 (325-005°) where there is a slight increase in the mean roughness length between wind speed Categories 1 and 2. Unfortunately, the dispersion in these data is so large that this trend is not statistically significant except in Group 1 (85-125°) and Group 3 (155-195°). In these groups the difference in the mean wind speed between Categories 1 and 3 is significant at the 99% level. A decrease in roughness lengths with increasing wind speed is consistent with the known characteristics of surfaces covered with certain types of vegetation; however, previous experimental data indicated a range in the values of  $\ln(z_0)$  of about 2.3 for a mean  $\ln(z_0)$  of -3.0 (Monteith, 1963).

Tables 7 and 8 show the variation of  $z_0$  with stability for wind speed Categories 1 and 2, respectively. Although the large dispersion in the data prevents any trend from being statistically significant, these data suggest that there is a rather large decrease in  $z_0$  between the stable and the neutral case but little further decrease in  $z_0$  between neutral and unstable. The greatest overall change in surface roughness with stability occurred in Groups 1 and 4 which are most directly influenced by a double change of terrain. For speed Category 1 profiles (Table 7) there is a very small increase in  $z_0$  from neutral to unstable in Groups 2, 3, 4, and 8. Panofsky and Petersen (1972) noted no decrease in  $z_0$  for the slightly unstable ten year mean profile (all

Table 6. Statistics for annual mean values of  $\ln(z_0)$  computed from neutral profiles for each wind speed category.

Group	10 Year Mean (Standard Deviation)		
	Wind Cat 1	Wind Cat 2	Wind Cat 3
1	-4.42 (2.58)	-7.18 (3.61)	-13.93 (8.70)
2	-10.25 (5.44)	-11.92 (5.66)	-16.04 (7.51)
3	-11.69 (7.29)	-14.77 (8.24)	-22.63 (7.04)
4	-8.04 (3.13)	-10.39 (3.85)	-15.08 (8.12)
5	-4.74 (1.97)	-5.68 (1.99)	-7.44 (3.19)
6	-2.22 (1.30)	-3.63 (2.36)	-4.94 (3.26)
7	-2.16 (1.30)	-2.77 (1.54)	-5.08 (4.42)
8	-5.04 (2.27)	-4.83 (2.45)	-6.96 (3.36)

Table 7. Statistics for annual mean values of  $\ln(z_0)$  computed from wind speed Category 1 profiles for each Richardson number category.

Group	10 Year Mean (Standard Deviation)		
	Stable	Neutral	Unstable
1	-2.47 (1.45)	-4.42 (2.58)	-4.81 (2.72)
2	-3.65 (1.86)	-10.25 (5.44)	-10.15 (5.07)
3	-4.80 (2.14)	-11.69 (7.29)	-11.65 (9.02)
4	-3.84 (1.37)	-8.04 (3.13)	-7.83 (3.35)
5	-3.23 (1.12)	-4.74 (1.97)	-4.86 (2.12)
6	-1.55 (0.90)	-2.22 (1.30)	-2.57 (1.41)
7	-1.26 (1.13)	-2.16 (1.30)	-2.37 (1.33)
8	-3.19 (2.09)	-5.04 (2.27)	-4.12 (1.76)

Table 8. Statistics for annual mean values of  $\ln(z_0)$  computed from wind speed Category 2 profiles for each Richardson number category.

Group	10 Year Mean (Standard Deviation)		
	Stable	Neutral	Unstable
1	-6.85 (3.02)	-7.18 (3.61)	-8.07 (3.62)
2	-7.83 (3.74)	-11.92 (5.66)	-13.89 (5.89)
3	-10.42 (4.69)	-14.77 (8.24)	-16.92 (9.78)
4	-8.01 (4.31)	-10.39 (3.85)	-10.76 (4.37)
5	-4.53 (2.04)	-5.68 (1.99)	-5.63 (2.65)
6	-3.11 (1.89)	-3.63 (2.36)	-3.25 (2.10)
7	-2.23 (1.54)	-2.77 (1.54)	-2.66 (1.30)
8	-4.07 (2.62)	-4.83 (2.45)	-4.93 (2.12)

speeds) in his Class B (Groups 2, 3, and 4) but a significant decrease in Class A (Group 1) and a small decrease in Class C (Groups 6, 7, and 8). The variation of  $z_0$  with stability is generally consistent with the results of van Hylickama (1970); however, his variation in  $z_0$  between stable and neutral was a 50% decrease and between neutral and unstable a 100% decrease for a  $z_0$  of 1 m for the neutral case.

Table 9 shows the variation of  $z_0$  over the seasons. As expected the relatively high roughness lengths occurred in summer and autumn to coincide with the seasonal cycle of vegetation growth. In Groups 2, 3, and 4 the largest roughness lengths occur in the winter which leads to speculation that occasional freezing of the narrow portion of Roskilde Fjord south of the tower results in a significant change in the structure of the internal boundary layer over a double change of terrain.

Table 9. Statistics for the ten year variation of seasonal mean values of  $\ln(z_0)$  computed from neutral mean seasonal profiles and then averaged over all speed categories.

Group	10 Year Mean (Standard Deviation)			
	Spring	Summer	Autumn	Winter
1	-6.22 (1.77)	-4.49 (1.47)	-5.28 (4.13)	-5.57 (4.51)
2	-11.47 (5.97)	-11.29 (5.52)	-12.39 (8.03)	-8.64 (10.53)
3	-12.52 (10.97)	-11.83 (9.37)	15.47 (10.75)	-10.82 (8.94)
4	-11.08 (6.62)	-9.42 (4.34)	-9.96 (6.89)	-7.39 (4.24)
5	-4.68 (3.31)	-5.13 (2.21)	-4.82 (2.55)	-5.49 (2.45)
6	-2.95 (2.13)	-2.90 (2.32)	-2.56 (1.86)	-3.19 (3.34)
7	-2.84 (1.86)	-2.56 (1.54)	-2.17 (1.46)	-3.15 (2.40)
8	-5.58 (4.31)	-4.90 (2.94)	-4.41 (3.21)	-5.92 (6.83)

## IX. CONCLUSIONS

During the planning stage of this study, it was assumed that a ten year record would result in a definitive characterization of the roughness lengths at Risø. Even if the non-equilibrium flow resulted in roughness lengths which were unrealistically small, it was expected that these  $z_0$ 's would at least be well behaved. However, this was not the case, and it appears impossible to estimate with any confidence the surface roughness lengths even from many mean profiles.

Until a better method of selecting equilibrium profiles is developed, estimates of surface roughness at Risø will have to be made on the basis of empirical equations relating aerodynamic roughness to the roughness element density and height.

The principal virtue of the results of Panofsky and Petersen (1972) was that their estimate of the  $z_0$ 's were reasonable in view of the physical description of the site. However, in lieu of a more detailed analysis of the variation of  $z_0$  when computed by their method, their results should be considered fortuitous rather than accurate.

The conclusions of this study are then threefold:

1. Averaging many neutral profiles over broad direction sectors does not always succeed in filtering out the effects of terrain inhomogeneities and Slade's hypothesis fails at a site as complex as the Risø site.

2. Panofsky and Petersen's large roughness lengths are apparently due to a method of selection which chooses only a small number of neutral profiles with large wind shear in the 7-23 m layer.
3. The roughness lengths at Risø cannot be determined to within one order of magnitude using normal profile techniques.

## BIBLIOGRAPHY

- Antonia, R. A., and R. E. Luxton. 1971. The response of a turbulent boundary layer to a step change in surface roughness. Part I. Smooth to rough. *J. Fluid Mech.*, 48, 721-761.
- Batchelor, G. K. 1953. Dynamic similarity of motions of a perfect-gas atmosphere. *Quart. J. Roy. Meteor. Soc.*, 79, 224-235.
- Bendat, J. S., and A. G. Piersol. 1971. *Random Data: Analysis and Measurement Procedure*. John Wiley & Sons, Inc. 407 pp.
- Bennett, C. A., and N. L. Franklin. 1954. *Statistical Analysis in Chemistry and the Chemical Industry*. John Wiley & Sons, Inc. 724 pp.
- Blackadar, A. K., and H. Tennekes. 1968. Asymptotic similarity in neutral barotropic planetary boundary layers. *J. Atmos. Sci.*, 25, 1015-1020.
- Blackadar, A. K., J. A. Dutton, H. A. Panofsky, and A. Chaplin. 1969. Investigation of the turbulent wind field below 150M altitude at the eastern test range. NASA Contractor Report, NASA CR-1410. 92 pp.
- Browne, N. E., H. D. Entreikin and G. E. Anderson. 1970. An analysis of the effect of terrain irregularities on turbulence and diffusion in the surface boundary layer. Final Report. Contract No. AT(30-1) 4140, USAEC. The Travelers Research Corp., Hartford, Conn. 148 p.
- Carl, D. M., T. C. Tarbell, and H. A. Panofsky. 1973. Profiles of wind and temperature over homogeneous terrain. *J. Atmos. Sci.* 30, 788-794.
- Clarke, R. H., A. J. Dyer, R. R. Brook, D. G. Reid, and A. J. Troup. 1971. The Wangara Experiment: Boundary Layer Data. Paper No. 19, Division of Meteorological Physics, CSIRO, Australia.
- Dabbert, W. F. 1968. Tower-induced errors in wind profile measurements. Annual Report. Grant No. DA-AMC-28-043-66-G24, ECOM, Fort Huachuca, Arizona, Univ. of Wisconsin. 91-104.

Deacon, E. L. 1949. Vertical diffusion in the lowest layers of the atmosphere. *Quart. J. Roy. Meteor. Soc.* 75, 89-103.

\_\_\_\_\_ 1953. Vertical profiles of mean wind in the surface layer of the atmosphere. *Geophysical Memoirs*, No. 91, Meteorological Office, London.

Dyer, A. J. 1963. The adjustment of profiles and eddy fluxes. *Quart. J. Roy. Meteor. Soc.*, 89, 276-280.

\_\_\_\_\_ 1971. Comment on: Conversion of profile difference quotients. *Boundary-Layer Meteor.*, 2, 130.

Echols, W. T. 1970. Modification in surface boundary layer wind structure with onshore flow. *Atmospheric Science Group, Report 23*, The Univ. of Texas at Austin. 59 pp.

Elliott, W. P. 1958. The growth of the atmospheric internal boundary layer. *Trans. Amer. Geophys. Union*, 39, 1048-1054.

Fichtl, G. H. 1968. Characteristics of turbulence observed at the NASA 150 m meteorological tower. *J. Appl. Meteor.*, 7, 838-844.

Fichtl, G. H., and G. E. McVehil. 1970. Longitudinal and lateral spectra of turbulence in the atmospheric boundary layer at the Kennedy Space Center. *J. Appl. Meteor.*, 9, 51-63.

Hanna, S. R., and H. A. Panofsky. 1969. Estimation of the 90 m wind from low-level observations. *Technical Note 93*, WMO Publ. No. 230, T. P. 123, 219-250.

Jenkins, G. M., and D. G. Watts. 1968. *Spectral Analysis and its Applications*. San Francisco, Holden Day, 525 pp.

Kitaygorodskiy, S. A., and Yu. A. Volkov. 1965. On the roughness parameter of sea surface and the calculation of momentum flux in the surface layer of the atmosphere above the water. *Izv. Atmos. Oceanic Phys.*, 1, 973-988.

Laikhtman, D. L. 1961. *Physics of the Boundary Layer of the Atmosphere* (English translation, 1964). Israel Program for Scientific Translations, Sivan Press, Jerusalem, 200 pp.

- Lettau, H. H. 1957. Computation of Richardson numbers, classification of wind profiles, and determination of roughness parameters. Exploring the Atmosphere's First Mile, Vol. I, H. H. Lettau and B. Davidson, Eds., New York and London, Pergamon Press, Inc., 328-366.
- 
- \_\_\_\_\_ 1969. Note on aerodynamic roughness parameter estimation on the basis of roughness element description. J. Appl. Meteor., 8, 828-832.
- Lumley, J. L. and H. A. Panofsky. 1964. The Structure of Atmospheric Turbulence. New York, Interscience, 239 pp.
- Monteith, J. L. 1963. Gas Exchange in plant communities. Environmental Control of Plant Growth, L. T. Evans, Ed., New York, Academic Press, 95-112.
- Morgan, D. L., W. O. Pruitt and F. J. Lourence. 1971. Analysis of energy, momentum, and mass transfers above vegetative surfaces. Research and Development Technical Report. Grant No. DA-AMC-28-043-68-G10, ECOM, Fort Huachuca, Arizona, Univ. of California. 128 pp.
- O'Brien, J. J. 1965. An investigation of the diabatic wind profile of the atmospheric boundary layer. J. Geophys. Res., 70, 2277-2290.
- Oliver, H. R. 1971. Wind profiles in and above a forest canopy. Quart. J. Roy. Meteor. Soc., 97, 548-553.
- Panofsky, H. A., and G. W. Brier. 1968. Some Applications of Statistics to Meteorology. The Pennsylvania State University.
- Panofsky, H. A., and E. L. Petersen. 1972. Wind profiles and change of terrain roughness at Risø. Quart. J. Roy. Meteor. Soc., 98, 845-854.
- Panofsky, H. A. 1973. Tower micrometeorology. Workshop in Micrometeorology, D. A. Haugen, Ed., Boston, Amer. Meteor. Soc., 151-176.
- 
- \_\_\_\_\_ 1974. The atmospheric boundary layer below 150 meters. Annual Review of Fluid Mechanics, Vol. 6, M. van Dyke, W. G. Vincenti and J. V. Wehausen, Eds., Palo Alto, Annual Reviews Inc., 147-177.

- Pasquill, F. 1949. Eddy diffusion of water vapour and heat near the ground. Proc. Roy. Soc. London, A198, 116-140.
- Paulson, C. A. 1970. The mathematical representation of wind speed and temperature profiles in the unstable atmospheric surface layer. J. Appl. Meteor., 9, 857-861.
- Petersen, E. L., and P. A. Taylor. 1973. Some comparisons between observed wind profiles at Risø and theoretical predictions for flow over inhomogeneous terrain. Quart. J. Roy. Meteor. Soc., 99, 329-336.
- Peterson, E. W., 1969. Modification of mean flow and turbulent energy by a change of roughness under conditions of neutral stability. Quart. J. Roy. Meteor. Soc., 95, 561-575.
- \_\_\_\_\_ 1974a. The Risø profiles: a study of wind and temperature data from the 123 m tower at Risø, Denmark. (Submitted to Quart. J. Roy. Meteor. Soc.).
- \_\_\_\_\_ 1974b. Personal communication.
- Plate, E. J., and C. W. Lin. 1966. Investigations of the thermally stratified boundary layer. Fluid Mech. Paper No. 5, College of Engineering, Colorado State University, Fort Collins, 40 pp.
- Plate, E. J. 1971. Aerodynamic Characteristics of Atmospheric Boundary Layers. USAEC, TID-25465, 190 pp.
- Remington, R. D., and M. A. Schork. 1970. Statistics with Application to the Biological and Health Sciences. Englewood Cliffs, Prentice-Hall, 418 pp.
- Sanders, L. D., and A. H. Weber. 1970. Evaluation of roughness lengths at the NSSL-WKY meteorological tower. ESSA Tech. Memo. ERLTM-NSSL 47, Norman, Oklahoma. 24 pp.
- Schlichting, H. 1968. Boundary Layer Theory, 6th Ed., New York, McGraw-Hill. 747 pp.
- Seginer, I., D. Rosenweig and D. Naveh. 1973. Flow around orientated porous obstructions III. Technion-Israel Inst. Tech., Dept. Agric. Eng. Publ. 189, 115 pp.

- Slade, D. H. 1969. Wind measurement on a tall tower in rough and inhomogeneous terrain. *J. Appl. Meteor.*, 8, 293-297.
- Stearns, C. R. 1968. Analysis of diabatic wind and temperature profiles. Grant No. DA-AMC-28-043-66-G24, ECOM, Fort Huachuca, Arizona, Univ. of Wisconsin. 1-56.
- Swinbank, W. C., and A. J. Dyer. 1968. Micrometeorological expeditions 1962-1964. Paper No. 17, Division of Meteorological Physics, CSIRO, Australia, 48 pp.
- Tanner, C. B., and W. L. Pelton. 1965. Potential evapotranspiration estimates by the approximate energy balance method of Penman. *J. Geophys. Res.*, 65, 3391-3414.
- \_\_\_\_\_ 1963. Basic instrumentation and measurements for plant environment and micrometeorology. Dept. of Soils Science, Univ. of Wisconsin, Madison.
- Tennekes, H., and J. L. Lumley. 1972. *A First Course in Turbulence*. Cambridge, The MIT Press, 300 pp.
- \_\_\_\_\_ 1973. The logarithmic wind profile. *J. Atmos. Sci.*, 30, 234-238.
- \_\_\_\_\_ 1973. Similarity laws and scale relations in planetary boundary layers. Workshop in Micrometeorology, D. A. Haugen, Ed., Boston, Amer. Meteor. Soc., 177-214.
- van Hylckama, T. E. A. 1970. Winds over saltcedar. *Agr. Meteor.*, 3, 217-234.
- Webb, E. K. 1965. Aerial microclimate. *Meteor. Monogr.*, Vol. VI, No. 28, 27-58.
- \_\_\_\_\_ 1970. Profile relationships: the log linear range, and extension to strong stability. *Quart. J. Roy. Meteor. Soc.*, 96, 67-90.
- Wyngaard, J. C. 1973. On surface layer turbulence. Workshop in Micrometeorology, D. A. Haugen, Ed., Boston, Amer. Meteor. Soc., 101-149.

## APPENDICES

## APPENDIX A

Derivation of the Logarithmic Wind Profile

The planetary boundary layer can be subdivided into four distinct layers each of which is governed by different physical conditions.

Platte and Lin (1966) describe each layer as follows:

1. The viscous sublayer near the wall where the mechanism for momentum exchange is entirely viscous.
2. A buffer region adjacent to the viscous sublayer in which both the viscous and the turbulent exchange processes are of similar magnitude.
3. The inner turbulent layer (surface layer) extending over the inner 15 to 20% of the boundary layer in which the shear stress is essentially constant.
4. The outer layer which extends to the edge of the free stream and in which buoyancy effects exceed shear effects.

Originally the logarithmic law had been derived by von Karman arguing from the local similarity of the profiles and shortly thereafter by Prandtl using the concept of mixing length (Schlichting, 1968).

The most elegant and rigorous derivation to date is found in Blackadar and Tennekes (1968), Tennekes and Lumley (1972), and Tennekes (1973) and is based on asymptotic similarity arguments.

Asymptotic similarity may be defined as scale-ratio independence of the large-scale description and of the small-scale description in nondimensional forms, chosen such that all functions remain finite as the independent parameter increases beyond limit.

The Navier-Stokes equations for the motion of an incompressible fluid with constant molecular viscosity,  $\mu$ , are:

$$\frac{\partial \tilde{u}_i}{\partial t} + \tilde{u}_j \frac{\partial \tilde{u}_i}{\partial x_j} = \frac{-1}{\rho} \frac{\partial \tilde{p}}{\partial x_i} + \nu \frac{\partial^2 \tilde{u}_i}{\partial x_j \partial x_j} \quad (\text{A-1})$$

where  $\nu$  is the kinematic viscosity,  $\nu = \mu / \rho$ , and  $\tilde{p}$ ,  $\tilde{u}_i$  are the instantaneous pressure and velocity, respectively.

Under a Reynolds decomposition (i. e.,  $\tilde{u} = U + u$ ,  $\tilde{p} = P + p$ , etc.), the equation for the time-averaged mean flow becomes the well known Reynolds momentum equation:

$$U_j \frac{\partial U_i}{\partial x_j} = \frac{1}{\rho} \frac{\partial}{\partial x_j} (-P \delta_{ij} + 2\mu S_{ij} - \rho \overline{u_i u_j}) \quad (\text{A-2})$$

where  $\overline{u_i u_j}$  is the Reynolds stress tensor and  $S_{ij}$  is the mean rate of strain tensor,  $[1/2(\frac{\partial U_i}{\partial x_j} + \frac{\partial U_j}{\partial x_i})]$ .

For atmospheric flows with a Cartesian coordinate system fixed to the earth so that it is rotating relative to an inertial reference frame with zero translational acceleration and the  $x_1$ ,  $x_2$  plane tangent to the earth so that the  $z$  axis is along the local vertical at latitude  $\phi$ , the Reynolds momentum equation becomes:

$$U_j \frac{\partial U_i}{\partial x_j} = \frac{1}{\rho} \frac{\partial}{\partial x_j} \{-P \delta_{ij} + 2\mu S_{ij} - \rho \overline{u_i u_j}\} - \epsilon_{ijk} f_j U_k - g \delta_{i3} \quad (\text{A-3})$$

where  $g$  is the effective gravity along the local vertical and  $f_j$ , the Coriolis parameter in the  $j^{\text{th}}$  direction, is twice the component of the earth's angular velocity in the  $j^{\text{th}}$  direction.

If we further assume that the flow is horizontal (i. e.,  $U_3 = 0$ ), homogeneous and of infinite extent so that the mean velocity profile is independent of its horizontal position (i. e.,  $\frac{\partial U_i}{\partial x_1}, \frac{\partial U_i}{\partial x_2} = 0$  and  $\frac{\partial P}{\partial x_1} = \text{const.}$ ), then the non-linear terms are suppressed, and Equation A-3 reduces to:

$$0 = \frac{-1}{\rho} \frac{\partial P}{\partial x_i} + \nu \frac{\partial^2 U_i}{\partial x_j \partial x_j} - \frac{\partial}{\partial x_j} \overline{u_i u_j} - \epsilon_{ijk} f_j U_k - g \delta_{i3} \quad (\text{A-4})$$

When the atmosphere is neutrally stratified (i. e., barotropic and adiabatic), the buoyancy term balances the vertical pressure gradient. If we align the  $x_1, x_2$  axes so that the surface stress is along the  $x_1$  axis, change to the more descriptive engineering notation, and replace partial differentials with total differentials wherever possible, then the component equations of motion are as follows:

$$0 = \frac{-1}{\rho} \frac{\partial P}{\partial x} + \nu \frac{d^2 U}{dz^2} - \frac{d}{dz} (\overline{uw}) + fV \quad (\text{A-5})$$

$$0 = \frac{-1}{\rho} \frac{\partial P}{\partial y} + \nu \frac{d^2 V}{dz^2} - \frac{d}{dz} (\overline{vw}) + fU \quad (\text{A-6})$$

The viscous term  $\nu \frac{d^2 U}{dz^2}$  is of order  $\nu \frac{u_*^2}{L^2}$  and, since  $\nu \frac{u_*^2}{L^2} = \frac{u_*^2}{L} \frac{1}{R_*}$ , we have:

$$\frac{d^2 U}{dz^2} \sim \frac{u_*^2}{L} \frac{1}{R_*} \quad \text{and} \quad \frac{d}{dz}(\overline{uw}) = \frac{u_*^2}{L} \quad (\text{A-7})$$

Therefore, for high Reynolds number flows ( $R_*$  is a friction Reynolds number), the viscous terms are negligible.

Equations A-5 and A-6 will next be applied to the PBL. If the flow outside the boundary layer is approximately steady, horizontal, and homogeneous in a horizontal plane, then we have the geostrophic wind case in the free stream above the boundary layer. In this case the pressure gradient is balanced by the geostrophic wind:

$$-fV_g = \frac{-1}{\rho} \frac{\partial P}{\partial x} \quad (\text{A-8})$$

$$fU_g = \frac{-1}{\rho} \frac{\partial P}{\partial y} \quad (\text{A-9})$$

The magnitude of the geostrophic wind is  $G = (U_g^2 + V_g^2)^{1/2}$  and  $z_0$  is simply some length scale for the surface layer proper. Therefore, the surface Rossby number  $Ro = G/fz_0$  is the external non-dimensional parameter for the flow in the boundary layer.

Substituting Equations A-8 and A-9 into Equations A-5 and A-6, the boundary layer equations become:

$$-f(V - V_g) = \frac{d}{dz}(-\overline{uw}) \quad (\text{A-10})$$

$$f(U - U_g) = \frac{d}{dz}(-\overline{vw}) \quad (\text{A-11})$$

The surface friction velocity,  $u_*$ , an internal parameter, is the appropriate velocity scale rather than the more obvious choice of  $G$ , the external parameter, because  $u_*$  is related to the internal dynamics of the turbulence through the surface stress,  $\tau_0 = \rho u_*^2$ , and  $u_*/G = f(\text{Ro})$  (Tennekes, 1974). If there are strong heat fluxes in the boundary layer, the vertical kinetic energy of the turbulence,  $1/2w^2$ , above the surface becomes large or small compared to the horizontal kinetic energy,  $1/2u_*^2$ ; however, for the neutral case  $w \sim u_*$  and  $u_*$  can be assumed to be the only velocity scale.

Length does not scale as simply. In the boundary layer there are always two length scales: (1)  $h = cu_*/f$ , the height of the boundary layer, ( $c$  is a constant of order unity) and (2)  $z_0$ , itself. For typical atmospheric conditions,  $h \approx 100$  m and  $z_0 \sim 0.01$  m and the ratio  $h/z_0$  is on the order of  $10^5$ , a rather large value.  $Z_0$  is the length scale of the small scale features close to the ground while  $h$  is the length scale needed to describe the large scale features characteristic of the whole depth of the boundary layer. Since  $h/z_0$  is not a function of height it must be a function of  $\text{Ro}$ , the external non-dimensional parameter. Therefore, when properly scaled, the non-dimensional equations of motion should be well behaved at  $\text{Ro} \rightarrow \infty$ . Scaling Equations A-10 and

A-11 with  $h = cu_*/f$  and  $u_*$  in the region  $z/z_0 \rightarrow \infty$ , the equations become:

$$\frac{-fh}{u_*} \left[ \frac{V-V_g}{u_*} \right] = \frac{d}{d(z/h)} \left[ \frac{\overline{-uw}}{u_*^2} \right] \quad (\text{A-12})$$

$$\frac{-fh}{u_*} \left[ \frac{U-U_g}{u_*} \right] = \frac{d}{d(z/h)} \left[ \frac{\overline{-vw}}{u_*^2} \right] \quad (\text{A-13})$$

therefore:

$$\frac{U-U_g}{u_*} = F_u \left[ \frac{zf}{u_*} \right], \quad \frac{V-V_g}{u_*} = F_v \left[ \frac{zf}{u_*} \right] \quad (\text{A-14})$$

where  $F_u$ ,  $F_v$  are well behaved functions (i. e., remain finite as  $Ro \rightarrow \infty$ ).

Closer to the surface but still far enough from the wall so that the roughness Reynolds number is very large (i. e.,  $z_0 u_*/\nu \gg 1$ ), when the equations of motion are scaled with  $z_0$  and  $u_*$ , we get:

$$\frac{-fz_0}{u_*^2} (V-V_g) = \frac{d(\overline{-uw})/u_*^2}{d(z/z_0)} \quad (\text{A-15})$$

$$\frac{fz_0}{u_*^2} (U-U_g) = \frac{d(\overline{-vw})/u_*^2}{d(z/z_0)} \quad (\text{A-16})$$

The terms  $(V-V_g)$  and  $(U-U_g)$  can be at most of order  $G$ ; therefore,  $(V-V_g)/u_*$  and  $(U-U_g)/u_* \sim G/u_* \approx 30$  for atmospheric cases. The ratio  $u_*/fz_0$  is the friction Rossby number  $Ro_f$ . In the limit as  $Ro_f \rightarrow \infty$ , the surface layer is to a first approximation a constant stress layer which does not feel the effect of the Coriolis force, and Equations

A-15 and A-16 become:

$$\frac{d(-\overline{uw}/u_*^2)}{d(z/z_0)} = 0; \quad \frac{d(-\overline{vw})/u_*^2}{d(z/z_0)} = 0 \quad (\text{A-17})$$

which upon integration becomes:

$$-\overline{uw} \propto u_*^2; \quad -\overline{vw} = 0 \quad (\text{A-18})$$

(The y component of the stress is zero because of our choice of axes.)

$$\frac{U}{u_*} = f_u(z/z_0); \quad \frac{V}{u_*} = 0 \quad (\text{A-19})$$

for the surface layer where  $z/z_0$  is finite because the wind profile has to scale on  $u_*$  and  $z_0$ .

If the sets of Equations A-14 and A-19 are matched in the layer  $z/z_0 \rightarrow \infty$ ,  $zf/u_* \rightarrow 0$ , as  $Ro \rightarrow \infty$ , the solution and all the derivatives in the vertical must agree. Differentiating with respect to height we have:

$$\frac{dU}{dz} = u_* \frac{dF_u}{dz} = f \frac{dF_u}{d(zf/u_*)} \quad (\text{A-20})$$

where  $F_u = F_u(zf/u_*)$  and

$$\frac{dU}{dz} = u_* \frac{df_u}{dz} = \frac{u_*}{z_0} \frac{df_u}{d(z/z_0)} \quad (\text{A-21})$$

where  $f_u = f_u(z/z_0)$ . Rearranging terms, Equations A-20 and A-21

become:

$$\frac{z}{u_*} \frac{dU}{dz} = \frac{z}{z_0} \frac{df_u}{d(z/z_0)} = \phi(z/z_0) \quad (\text{A-22})$$

$$\frac{z}{u_*} \frac{dU}{dz} = \frac{fz}{u_*} \frac{dF_u}{d(zf/u_*)} = \Phi(zf/u_*) \quad (\text{A-23})$$

We are looking for non-trivial solutions for  $\phi$  and  $\Phi$  as their arguments approach infinity (i. e.,  $\phi$  and  $\Phi$  should be asymptotically independent of all parameters or, in other words, constant); therefore, both equations reduce to the form:

$$\frac{z}{u_*} \frac{dU}{dz} = \frac{1}{\kappa} \quad (\text{A-24})$$

where  $\kappa$  is called von Karman's constant. Upon integrating Equation A-24 with respect to  $z/z_0$  and  $zf/u_*$ , there follows the familiar logarithmic wind profiles:

$$\frac{U-U_g}{u_*} = \frac{1}{\kappa} \ln(zf/u_*) + \text{const.} \quad (\text{A-25})$$

$$U/u_* = \frac{1}{\kappa} \ln(z/z_0) + \text{const.} \quad (\text{A-26})$$

The additive constant in Equation A-26 is very small, and it is usually absorbed into the definition of  $z_0$ .

The matched layer (inertial sublayer) only occurs when  $z/z_0 \rightarrow \infty$  and  $zf/u_* \rightarrow 0$  simultaneously. For this reason Blackadar and Tennekes (1968) have shown that it is not formally correct to force Equation A-26 to fit the boundary conditions at the surface ( $u = 0$  at  $z = z_0$ ) but

this issue is of minor importance since the parameter  $z_0$  is always chosen to conform to Equation A-26.

Derivation of the logarithmic wind profile in this manner emphasizes the fact that this equation does not apply to the surface layer proper (the region below about 1 meter) but only to the matched layer which links the surface layer proper to the outer layer.

Tennekes (1973) estimates that the upper limit of validity of the logarithmic law is at  $zf/u_* = 0.03$  (which is about 100 m under typical atmospheric conditions (Panofsky, 1972)). Furthermore, Tennekes (1973) concluded that the accuracy and usefulness of this equation is relatively insensitive to the constant stress assumption.

Complicating parameters which may possibly affect the slope and other features of the profile are thermal wind effects, inhomogeneities, non-stationary boundary conditions, and the presence of a vertical heat flux.

Up to this point  $z_0$  has been defined simply as the length scale of the surface layer where  $z/z_0$  is finite and  $u_*z_0/\nu \gg 1$ . Figure A-1 illustrates that the length scale of the turbulent eddies which are directly responsible for the drag on the rough surface should be scaled by some external parameter related to the size of the roughness elements. This is why the length scale  $z_0$  is properly called a roughness length.

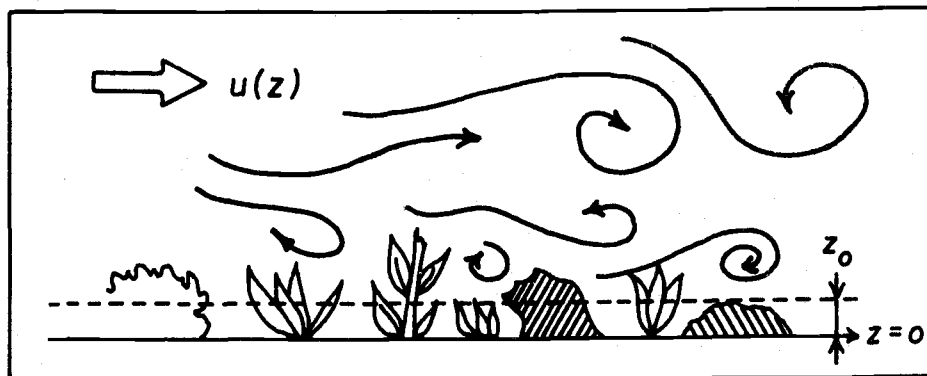


Figure A-1. The surface layer. After Tennekes, 1974.

## APPENDIX B

Analysis of Meteorological Data

Observed data representing physical phenomena such as the wind and temperature distributions at Risø can be classified as being either deterministic or random. A random data sample is drawn from an underlying population in such a way that every member of the population has the same probability for selection and the different units are selected independently. In this study, as in most other meteorological studies, it is necessary to use a certain period as the sample and then to consider this record to be one physical realization of a random process.

Random data are subdivided into stationary or nonstationary data. Data are stationary if the mean value is statistically constant.

Stationary random data can be further divided into ergodic or non-ergodic data. Data are ergodic if the average over an infinite number of realizations at a given time is equal to the average of a single realization over a sufficiently long period of time.

Ergodic data from an individual time series are stationary in the sense that the mean computed over time intervals does not vary from one interval to the next greater than would be expected due to the normal statistical sampling variation.

In view of the difficulties in demonstrating a priori that meteorological data are truly random, stationary, and ergodic the best technique to use in dealing with a long time series is to assume that the data are random and then see if analysis reveals any super-imposed deterministic effects.

The basis properties of discrete random processes are described by four types of statistical functions: (1) the standard deviation, (2) the autocorrelation function, (3) the probability density histogram, and (4) the power spectral density function.

Spectral methods are useful to analyze the frequency domain, but since they require a minimum of 500-1000 data points their use is precluded in this case and analysis has been confined to the temporal domain.

The number of annual and seasonal means is so small that the probability density histograms do not show anything that cannot be better described by the standard statistics (mean, standard deviation, kurtosis, and skewness).

The autocorrelation function for a sample of size  $n$  with mean,  $\bar{x}$ , and variance,  $s^2$ , is:

$$\rho(k) = \frac{\sum_{i=1}^{n-k} (x_{i+k} - \bar{x})(x_i - \bar{x})}{(n-1)s^2} \quad (\text{B-1})$$

where  $k$  is called the lag. It is useful to detect possible deterministic effects which might be masked by the random variations. If the data are truly random and stationary, the autocorrelogram will be that of "white noise". This is illustrated by Figure B-1 below.

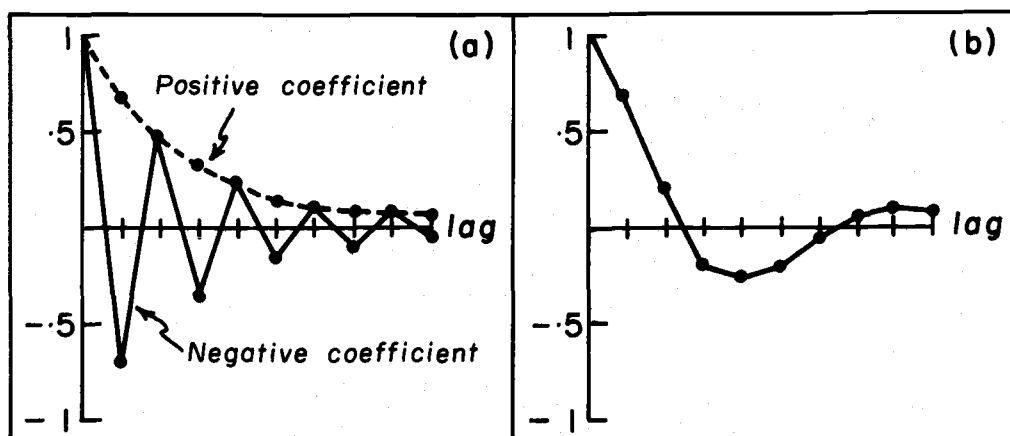


Figure B-1. Theoretical autocorrelograms for purely random data (white noise): (a) a discrete first order process,  $\rho(k) = \pm(0.7)^{|k|}$  and (b) a discrete second order process.

All individual profiles were selected for neutrality on the basis of the 7 m wind and then averaged over quarterly and annual periods. It follows from the central limit theorem that such means will themselves be normally distributed. The only constraint applied to the 23 m wind is that, for each individual profile, the 23 m wind must be greater than the 7 m wind. It is therefore reasonable to assume that the mean 23 m winds are also normally distributed. The actual mean wind data for both heights was usually negatively skewed and platykurtic (i. e.,

skewed towards high roughness values and having a distribution flatter than that of the normal distribution), but the sample size is too small for meaningful tests of this departure from normality.

It is a consequence of regression theory that the slope,  $\bar{b}$ , of a line through the mean  $\bar{U}_{23}$  and  $\bar{U}_7$  wind speeds will be normally distributed. In this study the  $\ln(z_0)$  was computed by a method equivalent to:

$$\overline{\ln(z_0)} = (\bar{U}_{23} + \bar{U}_7)/2\bar{b} - (\ln 23 + \ln 7) \quad (\text{B-2})$$

where  $\bar{b} = \bar{u}_*/\kappa$  is the mean slope. Hence,  $\ln(z_0)$  is a nonlinear function of three normally distributed variables and will not in general be normally distributed. However, if  $\ln(z_0)$  can be adequately represented by the linear terms of its Taylor series expansion, then:

$$\begin{aligned} \ln(z_0) \approx \overline{\ln(z_0)} + \frac{\partial \overline{\ln(z_0)}}{\partial U_{23}} (U_{23} - \bar{U}_{23}) + \frac{\partial \overline{\ln(z_0)}}{\partial U_7} (U_7 - \bar{U}_7) \\ + \frac{\partial \overline{\ln(z_0)}}{\partial b} (b - \bar{b}) \end{aligned} \quad (\text{B-3})$$

and  $\ln(z_0)$  will be approximately normally distributed (Bennett and Franklin, 1954).

Kitaygorodskiy and Volkov (1965) reanalyzed the profile data from several previous investigations. Using dimensional analysis rather than similarity theory, they were able to show that it was reasonable to assume that  $\ln(z_0)$  was normally distributed with sufficient

accuracy for meaningful statistical analysis.

Statistical analysis of the Risø data was done using SIPS, a statistical interactive programming system developed by the Oregon State University Department of Statistics and Computer Center.

## APPENDIX C

Typical Surface Roughness Lengths

The values of the roughness parameter,  $z_o$ , have been studied for the last 65 years. Typical values for natural surfaces may be found in the literature. There is only broad agreement in these data, probably because  $z_o$  is sensitive to the fine scale details of the structure of the underlying surface.

Table C-1. Data of Paeschke (1937)\*

Type of Surface	$z_o$ (cm)
Plane, snow covered	0.49
Grassy surface	1.73
Flat country	2.14
Low grass	3.20
High grass	3.94
Wheat	4.5
Tan and Ling:	3 to
	4.8
Beets	6.4

\*Quoted in Plate (1971)

Table C-2. Data of Laikhtman (1964)

Type of Surface	$z_o$ (cm)
Very smooth (snow, ice surface)	0.001
Meadow with grass of height up to 1 cm	0.1
Plain, sparse grass of height up to 10 cm	0.7
Plain, dense grass of height up to 10 cm	2.3
Plain, sparse grass of height up to 50 cm	5
Plain, dense grass of height up to 50 cm	9

Table C-3. Data of Deacon (1953)

Type of Surface	$z_0$ (cm)
Smooth mud flats	0.001
Smooth snow on short grass	0.005
Desert (Pakistan)	0.03
Snow surface, natural prairie	0.10
Mown grass:	
1.5 cm	0.2
3.0 cm	0.7
4.5 cm $\left\{ \begin{array}{l} u_2 = 2 \text{ mps}^* \\ u_2 = 6-8 \text{ mps} \end{array} \right.$	2.4 1.7
Long grass, 60-70 cm $\left\{ \begin{array}{l} u_2 = 1.5 \text{ mps} \\ u_2 = 3.5 \text{ mps} \\ u_2 = 6.2 \text{ mps} \end{array} \right.$	9.0 6.1 3.7

\* $u_2$  is the mean wind velocity at 2 meters

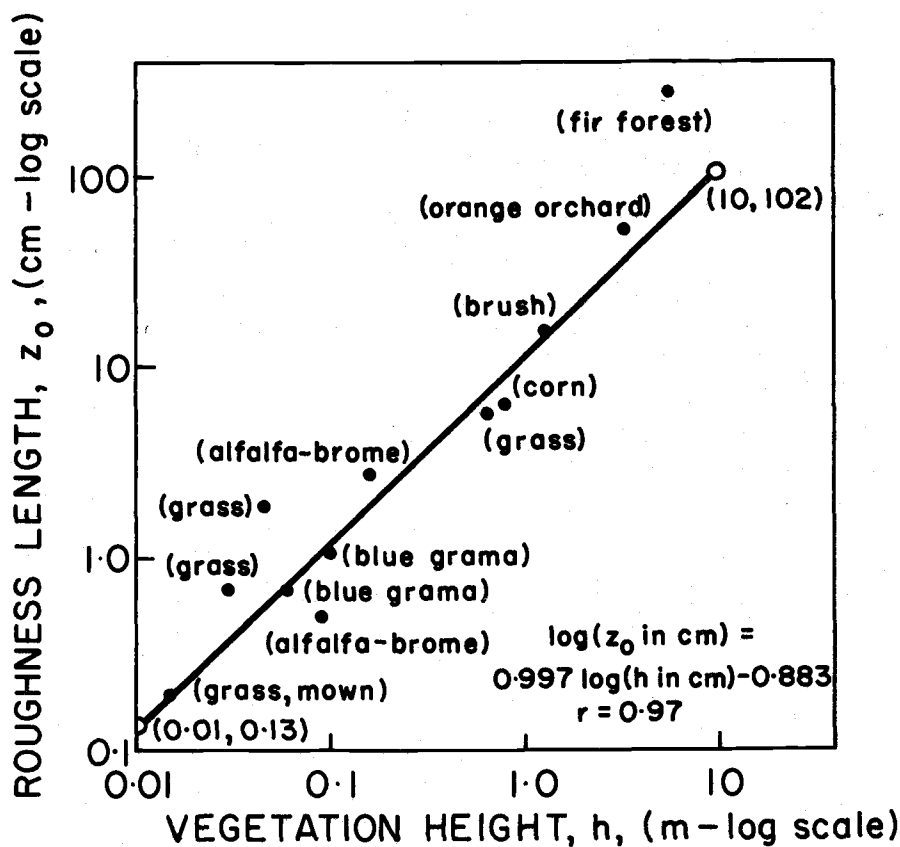


Figure C-1. Graph for estimating roughness lengths from vegetation height. After Tanner and Pelton (1960).